



IGS

S E S S I O N 6
A P P L I C A T I O N S

IGEX – A Regional Analysis of Data from the Southern Hemisphere

Micheal P. Stewart, Maria Tsakiri and Jinling Wang
Curtin University of Technology, School of Spatial Sciences
Perth 6845, Western Australia

Joao F. Galera Monico
Departamento de Cartografia, FCT/UNESP
Rua Roberto Simonsen 305 CEP 19060-900, Presidente Prudente, SP, Brazil

Abstract

This paper presents a regional treatment of data from sites operating in the Southern Hemisphere as part of the International GLONASS EXperiment (IGEX). GLONASS-only and GPS-only solutions have been computed for a network covering Australia, Antarctica and South America. The capabilities of GLONASS for regional geodetic positioning are demonstrated in the context of the existing GLONASS constellation and the IGEX experiment itself. The data processing strategies implemented in this preliminary GLONASS solution are also discussed.

Introduction

Five years after reaching full operational capability, GPS is used routinely for definition of regional control networks and for deformation analysis on regional and continental scales. Due to the relatively low cost of receivers and their superior portability, GPS has supplanted older, more cumbersome geodetic measuring techniques, such as VLBI and SLR, for all but the highest precision inter-continental measurements. Indeed, such is the strength of the global GPS network run by the International GPS Service (IGS), GPS contributed over 40% of the sites used in the realisation of the 1997 International Terrestrial Reference Frame (Boucher et al., 1999).

The flexibility afforded geophysical and geodetic researchers measuring regional crustal movements is offset to some extent by the inherent geometric weakness in the height component of GPS solutions. Most other GPS biases, such as orbital error, antenna phase centre variation, troposphere and tidal effects, are modelled explicitly by geodetic GPS data processing software suites. However, other receiver-dependent biases, such as antenna setup and local multipath effects, often remain. Therefore, it is not unusual for regional GPS solutions to be contaminated by small systematic errors. When attempting to resolve crustal motions at the millimetre level, these errors can become significant.

Establishing networks of continuously operating GPS reference stations (CORS) has proved to be the most effective technique for regional deformation monitoring. Error modelling of long data time series from such networks has allowed crustal motion

monitoring to reach unprecedented levels of precision. Accuracy of regional GPS networks is usually assessed in terms of internal precision of the GPS network, and agreement with independent geodetic positioning techniques such as SLR and VLBI. However, the luxury of CORS networks is not possible in all parts of the world where financial or logistical constraints may restrict geodetic monitoring to a series of episodic campaigns. Furthermore, the distribution of monitoring points on a CORS network may be too sparse to deliver significant deformation information. In such cases, episodic regional densification campaigns are usually required.

From a scientific point of view, the accuracy of regional, episodically observed, GPS networks is somewhat problematic. Primarily due to lack of external control, accuracy estimates tend to rely predominantly on the internal precision estimators given by GPS processing software. In ideal situations, GPS network solution coordinates can be compared with points in the network also observed by VLBI or SLR. The number of such points available worldwide is strictly limited, however, and these points are rarely available in practice. Another technique is to leave the coordinates of known stations (usually CORS sites) floating in the GPS network solution, and compare the 'recovered' coordinates of these stations with their known coordinates. This technique is limited by the number of CORS stations available to the network and can only give accuracy estimates at individual points.

It can therefore be argued that the accuracy estimation of regional GPS solutions would be more reliable if an independent set of coordinates could be derived for each point in the network. This possibility becomes more realistic with the availability of other global satellite-based positioning systems. This paper demonstrates the potential of the Russian Global Navigation Satellite System (GLONASS) to provide independent solutions for regional control networks and geodetic monitoring.

GLONASS for Regional Control Networks

The fundamental concepts behind the GLONASS system are very similar to GPS. In principle, GLONASS can be applied to regional positioning networks using similar processing techniques to those applied to GPS. The main reason GLONASS has not, to date, had any impact on regional control networks is mainly due to a worldwide lack of dual-frequency GLONASS receivers. The uncertainty in future funding for the GLONASS system, coupled with the incompleteness of the existing GLONASS constellation, has led to receiver manufacturers being understandably cautious about bringing high precision geodetic GLONASS receivers to market. Even though the GLONASS constellation can, at the moment, only be approximated to the GPS constellation of the late 1980s, surprisingly little work has been published of the suitability of GLONASS for long baseline processing. As an analogy, much of the pioneering work on GPS in the 1980s was carried out with a less complete GPS constellation than today's operational GLONASS constellation. It can therefore be expected that, as a system, GLONASS can today contribute to existing geodetic measurement techniques. The International GLONASS Experiment (IGEX) has provided

many research groups with the opportunity to apply existing regional GPS processing techniques to GLONASS observations.

The International GLONASS Experiment (IGEX, e.g., Willis and Slater, 1999) is the first global campaign of observations using the GLONASS satellite positioning system. It is run under the auspices of the International Association of Geodesy (IAG), International GPS Service (IGS), the International Earth Rotation Service (IERS) and the Institute of Navigation (ION). For the duration of the experiment, over 60 GPS/GLONASS receivers have been located at sites around the world (around a fifth of these in the Southern Hemisphere). Observations have been collected from GPS and GLONASS satellites at 30-second intervals, continuously from September 1998 until the present day.

A further aim of this study was to analyse the limited amount of IGEX data available in the Southern Hemisphere. Such a study would yield information on the logistical success of the IGEX experiment, the precision of IGEX precise orbits in the Southern Hemisphere, and the quality of raw Southern Hemisphere IGEX data.

Regional Observation Network and IGEX Data Availability

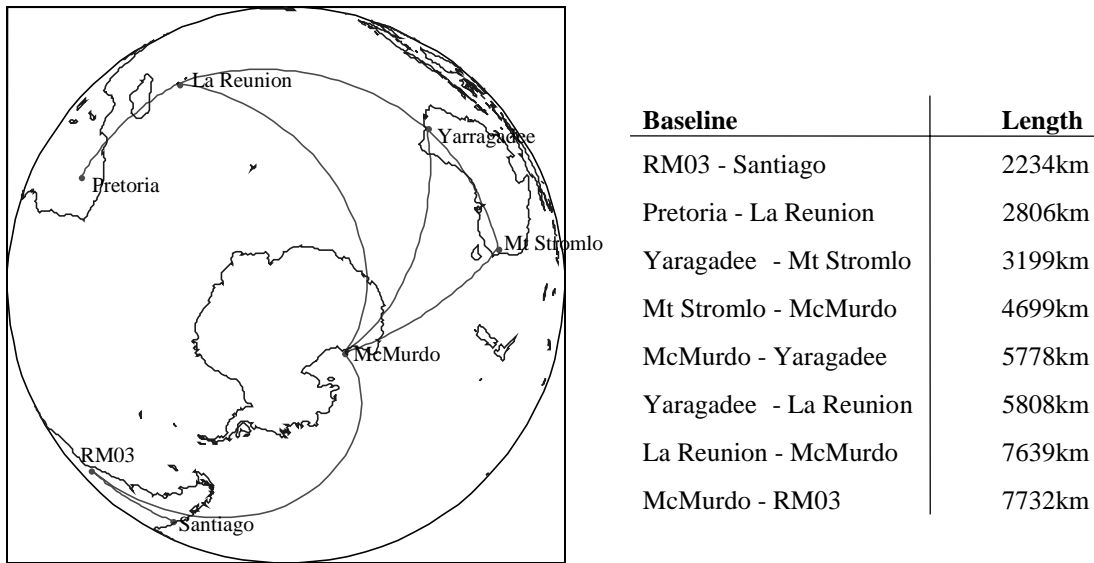
For this study, a subset of IGEX stations was selected, encompassing all continents in the Southern Hemisphere. A summary of IGEX stations and receiver types is shown in Table 1. By necessity, dual-frequency GLONASS observations were required at each station used in this study.

Table 1. Dual-Frequency IGEX Stations in the Southern Hemisphere

<i>station</i>	<i>location</i>	<i>receiver type</i>	<i>notes</i>
La Reunion	Indian Ocean	Ashtech Z18	
McMurdo	Antarctica	JPS Legacy	Available 16 th December 1998 – 6 th February 1999.
Pretoria	South Africa	3S R100/30T	No more than 2 GLONASS satellites observed with dual frequency at any one time.
RM03	Brazil	JPS Legacy	JD029, 047-054 only. Not an IGEX station.
Santiago	Chile	3S R100/40	Limited dual frequency GLONASS observations
Mt Stromlo	Australia	Ashtech Z18	
Yaragadee	Australia	Ashtech Z18	

Receivers from three different manufacturers (Ashtech, Javad Positioning Systems and 3S Navigation) were used at the seven stations distributed over Australia, Antarctica, South Africa and South America. Limitations on this Southern Hemisphere data set were

imposed due to the receiver at Crary Science Laboratory, McMurdo being only available for the duration of the Antarctic summer. Furthermore, the 3S receivers at Pretoria and Santiago only logged limited numbers of dual-frequency GLONASS observations due to restrictions in the numbers of channels in the receivers. These losses were offset to a small extent by the presence of a JPS Legacy receiver in Brazil (station RM03) for a few days in early 1999. The data set from this site is not part of the official IGEX data set, however.



Baselines are shown as great circles on the surface of the Earth

Figure 1. Southern Hemisphere GLONASS test network – processed baselines.

The final set of baselines processed in this study is shown in Figure 1. The length of baselines shown in figure 1 is not conducive to standard double difference data processing. On extremely long baselines, fewer satellites can be simultaneously observed by the stations constituting either end of the baseline. The correlation between observations, used to reduce atmospheric and orbital errors by the double differencing procedure, is extremely weak on long baselines, offsetting the advantages of applying the double difference processing procedure. The unavailability of the full GLONASS constellation further restricts the number of dual-frequency GLONASS observations available on the baselines for this study. The total number of days processed for each baseline and the average number of double difference dual-frequency observations for each baseline per day are given in Table 2.

Table 2. Number of Days Processed and Average Number of Double Difference GLONASS Observation Used Per Day

Baseline	Length (km)	Number of days processed	Average number of usable DD GLONASS observations per day
RM03 -Santiago	2234km	1	1009
Pretoria - La Reunion	2806km	4	273
Yaragadee - Mt Stromlo	3199km	4	789
Mt Stromlo - McMurdo	4699km	6	409
McMurdo -Yaragadee	5778km	7	1091
Yaragadee - La Reunion	5808km	7	847
La Reunion -McMurdo	7639km	5	278
McMurdo - RM03	7732km	1	490

It should be noted, that Table 2 represents the number of double difference observations actually used in the final GLONASS solutions (after removal of noisy data in the preprocessing phase and with an elevation masking angle of 20°), rather than the number of double difference observations physically observed.

The available IGEX data were divided into weekly segments. One baseline was allocated to each week and seven daily solutions were computed for each baseline. Allocation of one baseline per week ensured that separate baseline solutions were independent. Therefore, the baseline network could be subsequently subjected to a least squares network adjustment without considering baseline correlations. Furthermore, all weekly baseline repeatabilities could also be considered independent.

As can be seen from Table 2, data availability was variable at the IGEX stations in the Southern Hemisphere, with only two baselines managing a full complement of 7 daily solutions. In many cases, days of data were lost on one station or another, or too few valid observations were available to compute a solution on a particular day. For example, in GPS week 992, the receiver at Mt Stromlo provided only 13 hours of usable data per day, reducing the total number of observations available on the Yaragadee – Mt Stromlo baseline. In the same week, two days of data (julian days 40 and 41) were missing from the Yaragadee site. Lack of dual-frequency GLONASS data at Pretoria and Santiago has led to some difficulty in the connection of South America and South Africa to the remainder of the network. The preliminary analysis presented in this paper will consider results only from the closed network encompassing the sites at La Reunion, McMurdo, Yaragadee and Mt Stromlo.

Data Processing Strategy

Software

One of the fundamental aims of this study was to convert existing in-house data processing software to process long baseline GLONASS observations. The software in question (SWAG – South West Australia GPS software) is a derivative of the University of Nottingham's GAS (GPS Analysis Software) version 2.4 (Stewart et al., 1994). This software has been used in Australia for data processing of regional GPS networks in relation to the definition of the new Geocentric Datum of Australia, GDA_{1994.0} (Stewart et al., 1998).

For precise positioning, the SWAG software suite uses the standard static double difference processing algorithm (e.g., Bossler et al., 1980) in conjunction with IGS precise ephemerides, standard models for Earth body tides, ocean tide loading and atmospheric loading, as documented by McCarthy (IERS, 1996), and phase centre models as recommended by the IGS (Rothacher and Mader, 1996). On long baselines, the final GPS solution is computed using a linear ionospheric-free combination of L1 and L2 observables (e.g. Teunissen and Kleusberg, 1998). Wet tropospheric delay effects are modelled using a random walk stochastic process as discussed in (Dodson et al., 1996).

Considerations for GLONASS Data Processing

The main difference between GPS and GLONASS carrier phase observables is that whilst GPS satellites transmit on the same L-band frequencies, GLONASS satellites transmit on different, albeit similar, frequencies. The net result is that double differencing of GLONASS observations no longer removes some of the clock errors associated with the raw observations (e.g., Raby and Daly, 1994). A simple solution to this problem is to scale the GLONASS L1 and L2 observations from each satellite to a common frequency (e.g., Leick, 1998), prior to input into the GPS processing software suite. Scaling GLONASS observations to the GPS frequencies therefore can remove clock errors in the double differencing procedure but has two negative side effects. First, scaling will also scale the noise on the raw GLONASS observations. Second, the ambiguities and cycle slips of the scaled GLONASS observations are no longer integer in nature.

Whilst these side effects may be significant for short baselines, they are of less concern over longer baselines. The ionospheric-free linear combination of L1 and L2 for GPS also results in a noisier observable and in a situation where ambiguities and cycle slips are non-integer in nature. Scaling L1 and L2 GLONASS observations to the respective L1 and L2 GPS frequencies allows direct application of the linear dual-frequency ionospheric combination techniques to double difference GLONASS observations. As the scaling term from GPS to GLONASS are very close to one, little is lost by scaling the GLONASS observations to GPS frequencies.

One advantage for the analysis of IGEX Southern Hemisphere data presented in this paper has been the availability of precise GLONASS orbits computed by the IGEX

analysis centres at Berne, Potsdam, Frankfurt, JPL and the European Space Agency. These GLONASS orbits are referenced to ITRF/WGS84 and GPS time, rather than the GLONASS time system and GLONASS reference frame PZ90. In principle, however, raw GLONASS phase and pseudorange observations, when used in conjunction with IGEX precise ephemerides, can be post-processed using existing GPS software once they have been scaled to GPS frequencies.

Southern Hemisphere IGEX Data Processing for GLONASS Solutions

For the test data set, processing was undertaken without reducing antenna heights to their ground reference points, that is, baselines were processed from antenna phase centre to antenna phase centre. This strategy removed any uncertainty in the approximate coordinates of the IGEX points, some of which were provisional (for example, Yaragadee).

The solutions shown below represent CODE (Berne) orbits only. Of all processing centres, it was found that the CODE orbital files gave the maximum number of satellites with their associated clock errors. These satellite clock errors are not estimated, as with solutions from other processing centres, but are inserted in the orbital files from the GLONASS broadcast ephemerides. For Southern Hemisphere processing, satellite clock errors were not available for some satellite orbits from some processing centres. Lack of satellite clock estimates renders that orbit unusable in the SWAG software.

Results

Daily baseline repeatabilities are presented in Table 3. The extremely high variability on the Pretoria – La Reunion line is due to a lack of dual-frequency GLONASS observations (see table 2). The results on this baseline justify the decision not to process longer baselines to Pretoria. Repeatabilities of over 1m in baseline length on the baselines Mt Stromlo – McMurdo and La Reunion – McMurdo can be attributed to a lack of data due to receiver failure in the former case, and lack of data due to the extreme length of the baseline in the latter case. On the three remaining baselines, repeatabilities in baseline length are 37mm, 144mm and 320mm. Whilst these values represent repeatabilities at the 50 part per billion level or less, it is evident that lack of double difference GLONASS data due to long baselines and the incomplete GLONASS constellation are having a negative effect on the solutions. This is illustrated by the fact that the lowest repeatabilities are associated with stations on shorter baselines with more observations.

In terms of a regional treatment of GLONASS data, forming repeat one-day arcs into multi-arc solutions offered one way of offsetting the data availability problem. The stations La Reunion (REUN), Yaragadee (YARR), Mt Stromlo (STRR) and McMurdo (CRAR) were formed into a braced quadrilateral network of five independent 4- or 5-day arc baseline solutions (depending on data availability), representing data from GPS weeks 990 – 994, respectively. Because data for each baseline were taken from separate weeks of IGEX data, each baseline solution (and its associated covariance matrix) could be treated as an independent set of baseline observations in a standard minimally

constrained least squares network adjustment with Yaragadee held fixed (Figure 2). The adjustment was performed in GEOLAB version 2.4d. The resultant confidence regions are given in Table 4.

Table 3. Daily Baseline Repeatabilities (GLONASS only solutions)

baseline	Length (km)	No. days	σ_x (m)	σ_y (m)	σ_z (m)	σ_{length} (m)	σ_{height} (m)
Pretoria - La Reunion	2806	4	14.665	12.737	3.519	6.259	17.481
Yaragadee - Mt Stromlo	3199	4	0.146	0.169	0.076	0.037	0.214
Mt Stromlo - McMurdo	4699	6	0.916	0.376	1.043	1.192	0.447
McMurdo - Yaragadee	5778	7	0.352	0.177	0.201	0.144	0.241
Yaragadee - La Reunion	5808	7	0.211	0.208	0.274	0.320	0.133
La Reunion - McMurdo	7639	5	1.145	1.312	3.309	2.573	0.500

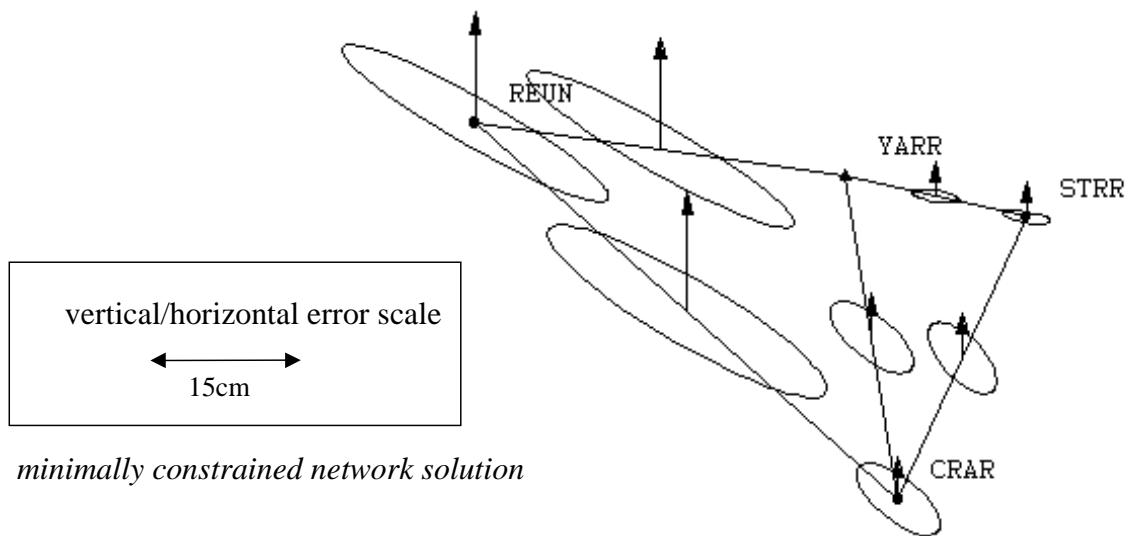


Figure 2. Minimally constrained adjustment of closed GLONASS Southern Hemisphere network (95% confidence).

Table 4. 2-D and 1-D Station Confidence Regions (95% confidence) for Figure 2

```

=====
GeoLab V2.4d                WGS 84                UNITS: m,DMS
=====
STATION          MAJOR SEMI-AXIS  AZ      MINOR SEMI-AXIS  VERTICAL
-----
CRAR              0.0654 129          0.0276           0.0560
REUN              0.1964 120          0.0302           0.1422
STRR              0.0311 100          0.0072           0.0453
=====

```

From Figure 2 and Table 4, the true potential of GLONASS carrier phase observations can be seen with horizontal 95% confidence regions at McMurdo (CRAR) and Mt Stromlo (STRR) being in the order of 6cm or less. Errors in the height component are of a similar magnitude. The adjusted coordinates at La Reunion (REUN) are of considerably lower quality than the other stations in the network, predominantly because even over a 5-day arc, the 7600km baseline between La Reunion and McMurdo was extremely weak geometrically.

For comparative purposes, the same multi-day arcs were processed with GPS observations. For GPS solutions, all processing models were identical to the GLONASS solutions, with the exception that IGS precise orbits were used. A similar network adjustment to that illustrated in Figure 2 and Table 4 was performed on the four independent GPS baseline solutions. The 95% confidence regions for the coordinate solutions for this adjustment are shown in Table 5.

Table 5. 2-D and 1-D Station Confidence Regions (95% confidence) for GPS Closed Southern Hemisphere Network

```

=====
GeoLab V2.4d                WGS 84                UNITS: m,DMS
=====
STATION          MAJOR SEMI-AXIS  AZ      MINOR SEMI-AXIS  VERTICAL
-----
CRAR              0.0432 122          0.0247           0.0529
REUN              0.0344 112          0.0032           0.0260
STRR              0.0213 88           0.0033           0.0267
=====

```

Comparing Table 4 and Table 5, the internal precision of the GPS network is seen to be stronger than the GLONASS network. This is unsurprising, given the likely superiority of IGS orbits for GPS in the Southern Hemisphere, and the greater amount of GPS data available. Figure 3 shows a comparison of the number of double difference observations processed for each four-day arc, for each GPS and GLONASS baseline. Figure 4 gives the a posteriori double difference observation noise estimates for each baseline and each satellite system.

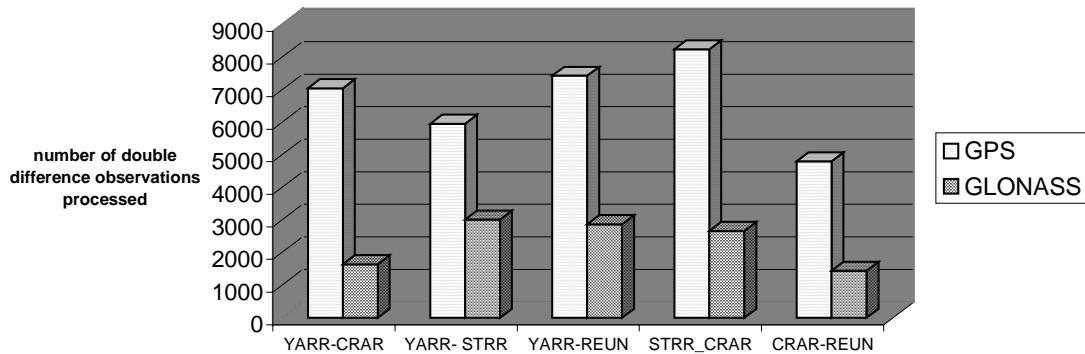


Figure 3. Number of double difference observations processed for 4-day arc GPS and GLONASS baseline solutions.

Figure 3 shows that well over twice as many double difference observations are available for the GPS solutions in comparison to the GLONASS solutions. This would appear to be the one limiting factor when comparing the internal precision of the GLONASS network to that of the GPS network, particularly on long baselines. In Figure 4, we see that the estimated noise on the raw double difference observations is comparable (around 5-6mm) for each solution. For this data set at least, the precision of raw GLONASS observations is not significantly different from that of GPS observations.

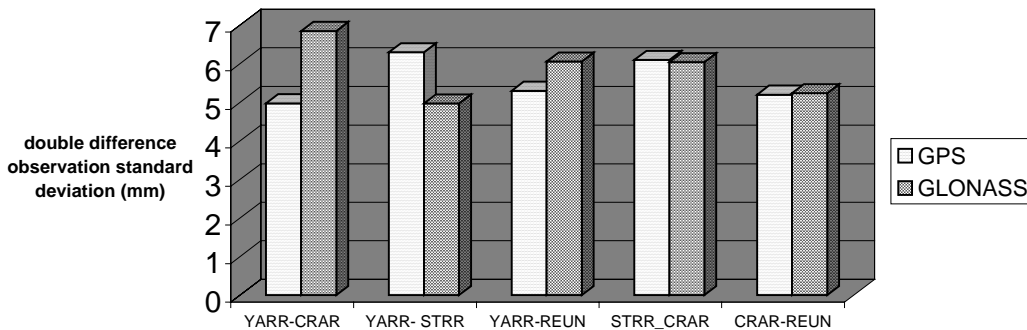


Figure 4. A posteriori double differences, standard deviations for GPS and GLONASS baseline solutions.

In both network adjustments for the GPS and GLONASS solutions, the coordinates of Yaragadee only were held fixed. Network orientation is essentially realised through (and hence dependent on) the fixed orbits. Whilst IGS precise orbits represent a reasonably accurate realisation of ITRF, IGEX orbits are correspondingly weaker due to fewer total stations being used in the orbit computation. This is particularly relevant to the Southern Hemisphere, where few stations observing GLONASS are available for GLONASS orbit

computation. Therefore, comparison of the final adjusted three-dimensional coordinates from the GPS and GLONASS solutions is more of an indication of the accuracy of the IGEX orbits in relation to the representation of ITRF through the fixed GPS orbits, rather than giving any indication on the suitability of GLONASS for regional solutions. The differences between the adjusted point solutions at each site (and associated errors) are given in Table 6, where the orientation of the networks is shown to be comparable at the 5 –10cm level. The exception is a 20cm rotation about the x and z components (predominantly the height component) at the Antarctic station of McMurdo (CRAR). This rotation is difficult to explain on the basis of this one data set, although lack of available tracking stations will cause IGEX orbits to be weaker in the higher latitudes of the Southern Hemisphere.

Table 6. Difference Between Network Adjusted 3-D Geocentric Station Coordinates (GPS – GLONASS)

station	dx (m)	σ_{dx} (m)	dy (m)	σ_{dy} (m)	dz (m)	σ_{dz} (m)
CRAR	-0.2063	0.0238	0.0368	0.0310	-0.2125	0.0356
REUN	-0.0466	0.0654	0.0246	0.0727	-0.0371	0.0517
STRR	-0.0348	0.0155	-0.0752	0.0221	0.0658	0.0155

Comparison of adjusted baseline lengths gives more of an indication of the quality of the GLONASS network solution in relation to the GPS network solution. Baseline length comparisons are shown in Table 7.

Table 7. Comparison of Adjusted Baseline Lengths for GPS and GLONASS Network Solutions

baseline	GPS length (m)	σ_{GPS} (m)	GLONASS length (m)	$\sigma_{GLONASS}$ (m)	GPS - GLONASS (m)	GPS - GLONASS error (m)
CRAR-REUN	7639012.416	0.022	7639012.237	0.068	0.179	0.071
CRAR-STRR	4698509.709	0.021	4698509.730	0.027	-0.021	0.034
CRAR-YARR	5778302.223	0.020	5778302.217	0.025	0.006	0.032
REUN-YARR	5808019.484	0.011	5808019.535	0.064	-0.051	0.064
YARR-STRR	3199303.727	0.010	3199303.661	0.016	0.066	0.019

In Table 7, the uncertainty in the GLONASS baseline lengths from the network adjustment to La Reunion (REUN) can be attributed to the effect of the weak baseline solution for McMurdo (CRAR) – La Reunion. This, in turn, weakens that part of the network. Notwithstanding the CRAR-REUN baseline, baseline length agreement is in the order around 5cm.

Discussion

It must first be emphasised that the multi-day arc solutions for both the GPS and GLONASS solutions are sub-optimal for the baseline lengths under consideration. The general precision of GPS baseline length solutions (in the order of 1-2cm) is little more than can be expected for precise ephemerides. Neither were antenna phase centre models applied, nor were ocean tide loading coefficients available at La Reunion and Mt Stromlo. Full rigorous modelling of these error sources would undoubtedly yield better results. As discussed previously, the merits of using double differencing on baselines of up to 7600km could also be said to be somewhat doubtful.

However, the aim of this study is to give an indication of the potential capabilities of GLONASS over long baselines. The striking aspect of the results presented is that over baselines of between around 3100km and 7600km in length, GLONASS solutions have been achieved which are comparable in precision to those achieved with GPS solutions. The agreement between GPS and GLONASS is at about the 0.01ppm level, which is similar to the internal precision of the individual network solutions. These results have been achieved with a sub-optimal GLONASS constellation. Given that IGEX orbits could one day be improved to a level approaching IGS orbital precision, the potential benefits of GLONASS for regional geodetic positioning are clear. Regional high precision GLONASS solutions are achievable with existing hardware.

Furthermore, the results vindicate the processing strategy adopted for GLONASS observations. For long baselines, scaling GLONASS observations to the GPS L1 and L2 frequencies is a simple and relatively straightforward modification to geodetic processing software. Obviously, the results presented are also reliant on the availability of GLONASS precise orbits. The CODE orbits used in this study resulted in an agreement in the orientations of the minimally constrained GPS and GLONASS adjusted networks at the 5 – 10 cm level.

Conclusions

GLONASS double difference carrier phase observations have been demonstrated to be comparable in precision to GPS for long baselines. Long baseline GLONASS solutions processed with precise ephemerides should be able to achieve similar precisions on regional networks to those routinely achieved with GPS. Given a full constellation, it would appear that GLONASS could be used as a simultaneous, yet independent, operating system for geodetic positioning. In the absence of a full GLONASS constellation, even on very long baselines, GLONASS can still deliver important additional information. However, until the future of the GLONASS system is politically secure, the emphasis is more likely to shift to augmenting GPS with the few GLONASS satellites available.

In the Southern Hemisphere, the IGEX campaign suffered from a lack of dual-frequency GPS/GLONASS stations. Overall, however, IGEX provided a long, high quality data set, demonstrating a capability to delivery GLONASS raw observations and precise orbits, to

users worldwide. If (or when) included within the IGS framework, other global navigation satellite systems will be able to substantially improve on the reliability and capabilities of the existing IGS GPS network.

References

Bossler, J. D., C.C. Goad and P. L. Bender (1980). Using the Global Positioning System (GPS) for Geodetic Positioning, *Bulletin Geodesique*, Vol. 54, pp. 553-663.

Boucher C., Z. Altamimi, P. Sillard (1999). The 1997 International Terrestrial Reference Frame (ITRF 1997), IERS Technical Note 27, Observatoire de Paris, Paris.

Dodson, A. H., P. J. Shardlow, L. C. M. Hubbard, G. Elgered, P. O. J. Jarlemark (1996). Wet Tropospheric effects on precise relative GPS height determination, *Journal of Geodesy*, Vol. 70, No. 4, pp. 188 – 202.

IERS (1996). IERS Conventions, IERS Technical Note 21, D. D. McCarthy (ed.), Observatoire de Paris, Paris.

Leick, A. (1998). GLONASS Satellite Surveying. *Journal of Surveying Engineering*, Vol. 121, pp. 91-99.

Rothacher, M., G. Mader (1996). Combination of Antenna Phase Centre Offsets and Variations: Antenna Calibration Set IGS_01. IGS Central Bureau (<http://igsceb.jpl.nasa.gov>)

Raby P. and P. Daly (1994). Surveying with GLONASS: Calibration, Error Sources and Results, *Proceedings 3rd International Symposium on Differential Satellite Navigation Systems*, Canary Wharf, London, UK, April 18-22, 1994.

Stewart, M. P., G. H. Ffoulkes-Jones, W. Y. Ochieng (1994). GPS Analysis Software (GAS) Version 2.2 User Manual, *Monograph*, University of Nottingham, 158pp.

Stewart M. P., H. Houghton, X. Ding (1998). The Statefix West Australian GPS Network, in *Advances in Positioning and Reference Frames*, F. K. Brunner(ed.), International Association of Geodesy Symposia, Vol. 118, Springer-Verlag.

Teunissen, P. J. G., A. Kleusberg (1998). GPS Observation Equations and Positioning Concepts, in *GPS for Geodesy*, P. J. G. Teunissen and A. Kleusberg, Eds., pp.188-229, Springer-Verlag.

Willis, P., J. Slater (1999). International GLONASS Experiment (IGEX-98), in *IGS 1998 Annual Report*, Jet Propulsion Laboratory, California Institute of Technology, Pasadena, California, JPL Publication 400-838.

PZ-90 GLONASS to ITRF Transformation as a Result of IGEX-98 Laser Tracking Campaign

Vladimir V. Mitrikas, Sergey G. Revnivikh

GEO-ZUP Company, 12 Ochyabrsky Boulevard, Korolyov of Moscow reg., Russia

Vladimir D. Glotov, Mikhail V. Zinkovski

Russian Mission Control Center, 2 Pionerskaya Street, Korolyov of Moscow reg., Russia

Abstract

One of the main targets of the International GLONASS Experiment (IGEX) was the determination of the transformation parameters between GLONASS and GPS reference frames PZ-90 and WGS 84. IGEX has allowed the application of different methods to find this transformation because code and phase measurements with the broadcast ephemeris data were collected from a number of receivers, and additionally 8 GLONASS satellites were permanently tracked by the international laser observatory network.

Indeed, the experiment was limited to half a year only. This is not a long term to investigate all the features of the transformation because it is not stable as it was shown in (Mitrikas et al., 1998). In that work, determination of the transformation parameters was done by comparison of post-processed ephemerides from the GLONASS System Control Center (SCC) with the ephemerides of two GLONASS satellites computed in the Russian Mission Control Center (MCC) from the laser data collected from the whole laser network since Autumn 1995. However that work used the post-processed ephemeris instead of actually being transmitted. Strictly speaking then, there is no evidence that the transformation parameters determined are free from any possible systematic differences between transmitted and post-processed SCC ephemeris. IGEX provided an extremely good opportunity to check the previously-obtained transformation. Merging together the new results and the results obtained in 1997-98, the transformation from PZ-90 GLONASS can be monitored for a period of 3.5 years. This is quite a long period from which to draw conclusions about the behavior of the transformation.

Orbits of eight GLONASS satellites in The International Terrestrial Reference Frame 1994 (ITRF94) have been computed from the laser data in MCC. Orbits of the same satellites in PZ-90 have been compiled from the real navigation messages collected in the frame of IGEX-98. Additionally, orbit positions of three GLONASS satellites have been calculated by averaging the post-processed ephemerides provided from SCC applying the procedure used in (Mitrikas et al., 1998). This was done for the comparison of the transformation parameters based on the broadcast and post-processed data in PZ-90.

As a result the transformation parameters between PZ-90 GLONASS and ITRF94 have been determined for the complete six month period of IGEX. It has been confirmed that the transformation is highly correlated with the difference between the Earth Orientation

Parameters (EOP) used in regular GLONASS Orbit Determination (OD) and final International Earth Rotation Service (IERS) values. The values obtained have been compared to the earlier work. Despite the difference in the translation of the origin along X and Y axes, it should be postulated the coincidence of the results.

Introduction

Obviously there is no need to substantiate the importance of the transformation between reference frames implemented by Space Navigation Systems (SNS) GLONASS and GPS. The problem has been widely discussed in particular at ION Meetings since 1995 (Mitrikas et al.,1998; Misra et al.,1996; Rossbach et al.,1996). All the results reported in the mentioned papers are similar: the main difference between the reference frames is concentrated in the rotation around the Z-axis and it has the value near 0.35 sec of arc which corresponds to 11 m along the equator. It must be noticed that the results above have been obtained by different methods - orbit comparison (Mitrikas et al.,1998; Misra et al.,1996) and ground receiver position comparisons (Rossbach et al.,1996). Of course one can easily find some difference between the parameters determined, but as it was explained in (Mitrikas et al., 1998), the major source of the differences is instability of the transformation with time. Hence, the results were much affected by parameter fluctuations because the investigations (Misra et al.,1996; Rossbach et al.,1996) covered a very limited time span.

In fact, none of the transformations has been adopted as a standard. Probably the main reason was that the Topographic Service of the Ministry of Defense of The Russian Federation (TSRMD), which was responsible for the PZ-90 solution, has reported completely different set of transformation parameters between PZ-90 and WGS 84 (Galazin et al.,1997; Bazlov et al.,1999). In practice, one who proposes some reference frame for the common use should describe how it is related to ITRF or at least to any well known reference frame. Such work for instance is supported for WGS 84 by the National Imagery and Mapping Agency (NIMA) (formerly DMA) (Malys and Slater,1994; NIMA,1997). So formally the transformation reported by TSRMD must have been the most accurate. Indeed those parameters differ from others too much because for years TSRMD declared the difference between PZ-90 and WGS 84 to be considerably less than that determined by other investigations (Mitrikas et al.,1998; Misra et al.,1996; Rossbach et al.,1996). The most interesting fact in this story is that perhaps all the researchers are right.

The essence of the problem is in the difference between clear scientific PZ-90 and its implementation via GLONASS. This question was partially described in (Mitrikas et al., 1998). So one should separate between PZ-90 and PZ-90 GLONASS reference frames when speaking about the transformation. But from the user point of view it is of no matter how the clear PZ-90 is related to ITRF. Everyone wants to know how to recalculate the GLONASS ephemerides to use them with other navigation systems. Hopefully IGEX-98 will end the misunderstanding and at least preliminary transformation parameters from PZ-90 GLONASS to ITRF and WGS 84 will be recommended.

The other feature of PZ-90 GLONASS is its instability in time. Probably it is caused by old models and algorithms used in the SCC routine software (SW). GLONASS uses its own values of polar motion (PM) determined from regular two-way range measurements. When the GLONASS reference frame was adjusted in 1987, EOP values were fixed to IERS (BIH at that time) values. Since then SCC uses its own PM values determined in the corresponding subsystem. As it has been shown in (Bykhanov, 1996), the difference between GLONASS PM and IERS PM grew up permanently. At the moment it includes a shift of the averaged pole and long term fluctuations.

In the regular SW, satellite state vectors are solved for in the inertial reference frame. In the orbit determination, the angle between the orbit plane and the instantaneous rotation axis of the Earth is determined confidently because usually the measurements are well distributed in the inertial reference frame. However when the satellite positions are transformed to the terrestrial reference frame, the PM errors influence the result. That is why all distributed ephemeris data are affected by GLONASS PM errors.

The current amplitude of GLONASS pole variations around the IERS pole is ± 0.030 sec of arc for each component. Moreover, there is a bias of GLONASS Yp component of 0.010-0.015 sec of arc. From the user point of view such an effect causes a drift of coordinate solutions even assuming all other error sources such as ionosphere, troposphere, multipath, ephemeris, and clocks are zero. In other words the same points have different coordinates at different times. The error of positioning due to wrong PM depends on the user's geographic coordinates and for some regions can exceed 1.5 m. Such fluctuations can be completely ignored from the point of view of system specification, but they are important as a scientific aspect of transformation parameter determination.

Basically the transformation parameters can be determined by two approaches:

- use of navigation receivers (GLONASS receivers on WGS 84 sites, GPS on PZ-90 sites or combined receivers)
- use of satellite coordinates represented in both frames.

Before IGEX-98, perhaps a lack of GLONASS receivers was the main problem in the implementation of the first approach. However, at least one effort was reported long before IGEX (Rossbach et al., 1996). Unfortunately due to a very short campaign and limited to a European distribution of the GLONASS receivers, it did not produce a very accurate solution. The first approach was also used in the determination of the transformation made by TSRMD (Bazlov et al., 1999). Here GPS receivers have been installed on PZ-90 sites. But despite the longer duration of the campaign and better geometry, the reported parameters were adjusted to clear PZ-90 instead of its GLONASS interpretation. In essence, the use of receivers is preferable to the comparison of satellite coordinates because it deals directly with the user positions. However the guaranteed solution became possible as a result of IGEX-98 campaign only. Due to variations of PZ-90 GLONASS, either a relatively long time period should be considered for the proper recommendation of the standard parameters or transformation parameters should be determined as functions of time. The second idea does not seem to be very attractive

because the change of parameters with time is about one order of magnitude less than their values.

According to a joint agreement of the National Aeronautics and Space Administration (NASA) and Russian Space Agency (RSA), the International Laser Ranging Service (ILRS) permanently tracks two GLONASS satellites located in different orbital planes. This campaign involves more than 25 stations, and enough data for precise orbit determination have been available since November 1995. That is why RSA funded the investigations of the transformation from PZ-90 GLONASS to ITRF by application of the orbital method. That work covered the period until June 1997. In 1998 it was decided to continue the investigation in the frame of IGEX-98. For this purpose laser-based orbits computed in MCC have been compared to both the transmitted ephemeris and post-processed or averaged ephemeris based on the data from GLONASS SCC. The procedure for the preparation of post-processed satellite positions was completely identical to that in (Mitrikas et al., 1998). Such an approach allowed 3.5 years monitoring of the transformation parameters.

Laser-based Orbit

The procedure of the GLONASS orbit determination has been described in (Mitrikas et al., 1998). Anyone who is interested in more details of OD should read (Glotov et al., 1999). Only a general description of MCC OD is presented in this paper.

The software for GLONASS OD was developed as a result of a joint activity of MCC and GEOZUP Company in 1996 and since that period there have been no major changes to it. The motion model combines the model used in MCC for the processing of geodetic satellites Etalon-1,2 with the GLONASS solar pressure model developed in GEOZUP Company. The initial information for GLONASS modeling was issued by NPO PM (Krasnoyarsk) which has designed all of the GLONASS satellites. These data as well as navigation antenna phase centers and retroreflector coordinates in the body-fixed reference frame were widely distributed by GEOZUP to all interested persons via IGEXMail. Despite this, the description of the GLONASS satellite did not contain all the necessary data to build a high-accuracy model; the missing information, such as reflectivity, adsorption and diffusion, was assumed to be similar to the Meteor-3 spacecraft. This approach was based on the rich experience in tracking data processing that had been accumulated by GEOZUP Company.

Station positions and velocities used in GLONASS OD have been adjusted in the SSC(GZ)98L01 solution based on laser data from geodetic satellites Lageos and Lageos-2. To implement ITRF94 station coordinates, EOP have been fixed to IERS final values when tracking station coordinates and biases were solved for. This solution was successfully used in MCC for one year for the routine determination of PM and Length of Day (LOD) in the frame of cooperation with IERS.

GLONASS orbit determination itself was carried out on 8.5 days almost independent arcs formed in such a way that each arc started exactly 8 days after the beginning of the previous one. The duration of 8.5 days was used to avoid possible tracking data holes on

the boundary between consecutive arcs. This OD scheme was selected as a result of a special investigation (Mitrikas et al., 1998). It allowed orbit accuracy estimation by comparison of two neighboring arcs and by projection of the current tracking residuals on the previous predicted orbit. Certainly this procedure also included prediction errors. Automatic and partial manual filtering of data outliers was performed before the final orbit obtaining. As in 1995-97, despite the fact that many stations took part in the campaign, most of the collected measurements were concentrated in about 5 regions: the Western and Eastern US, Europe, Australia and Hawaii. Moreover, data from some relatively new stations have not been included in the OD because of the absence of their precise positions in the GZ98L01 coordinate solution. In particular, this affected station 7849 (Stromlo, Australia), which was of some concern, because of the very limited number of facilities in the Southern hemisphere. The same problem existed for the Keystone stations in Japan because most of them started operations in the autumn of 1998.

The total number of stored passes per satellite is a little better than during the tracking campaign of two GLONASS satellites in 1995-97. However, taking into account corrupted data and data not involved due to the absence of station coordinates, the average amount of laser data used is about 2.5 passes per day for each satellite. Finally, excluding a few parts of orbits, the following Root Mean Square (RMS) values have been calculated for the GLONASS satellites:

<u>Sat N</u>	<u>Plane</u>	<u>Total</u>	<u>Radial</u>	<u>Along-track</u>	<u>Cross-track</u>
68	1	1.67 m	0.20 m	0.88 m	1.41 m
69	1	2.75 m	0.28 m	0.96 m	2.56 m
70	1	1.77 m	0.24 m	0.88 m	1.51 m
66	2	3.25 m	0.27 m	2.30 m	2.28 m
79	2	2.59 m	0.30 m	1.96 m	1.67 m
62	3	2.34 m	0.22 m	0.97 m	2.12 m
71	3	2.43 m	0.18 m	1.23 m	2.09 m
72	3	2.97 m	0.26 m	1.09 m	2.75 m

Here each number has been computed from the differences between the positions of the satellite in the neighboring solutions. Averaging was done with a 30 minute step over a 1-day interval from the beginning of each solution. It is important that these numbers correspond to the boundaries of arcs. Basically orbit error can be considered as a random value. Taking into account these facts, we can conclude that the actual orbit accuracy should be at least 1.5 times better. In any case, this is worse than the accuracy of phase-based orbits. But in fact too long a time interval (8.5 days) was used because of poor coverage of orbits by laser data. It should be mentioned that the solar panel orientation of GLONASS satellites is hard to model for long periods.

There is a very large difference compared to the work done by (Mitrikas et al., 1998). Here all OD has been managed by the routine MCC service while in the earlier work, all orbits were computed by GEOZUP Company in the investigation mode. Because of operator errors and the fact that the OD SW was not suited for fully automatic processing,

in some cases the quality of the obtained orbits is worse than it could be. Unfortunately this fact was recognized too late to re-compute all the required arcs for this work. That is why an additional analysis has been performed for each satellite to retain only those parts of the orbit where the accuracy was high enough. So a significant number of days without guaranteed orbits have been excluded.

In fact, even an absolutely correct OD could not significantly increase orbit accuracy because the OD was based on too long arcs and an insufficient amount of data. Probably the number of rejected days could be reduced. On the other hand, clearly the quality of the orbit in ITRF94 is better than that of the of broadcast ephemeris. So any unexpected results should be due to the quality of the transmitted ephemeris rather than the quality of the ITRF orbits.

Regular and Post-Processed Averaged Regular Orbit

First, one should distinguish between the broadcast regular orbit and the so-called averaged regular orbit. The broadcast regular orbits have been compiled from the data collected by the IGEX network. The averaged regular orbits have been obtained in GEOZUP on the basis of information from SCC.

In order to avoid propagation errors, the broadcast orbit of each satellite was represented as a set of its positions in PZ-90 GLONASS with a 30-minute time step at 15 or 45 minutes every hour. Due to the GLONASS data structure, in this case there was no need to carry out an integration. Indeed not all the broadcast ephemeris data have been collected by IGEX network especially at the beginning of the campaign. Data omissions were in the southern hemisphere but those regions are quite problematic for the laser data also.

The scheme of the averaged or improved orbit generation from SCC data was described in (Mitrikas et al., 1998), so this paper reviews only the major aspects. The standard SCC OD scheme utilizes a 17-revolution (8-day) navigation time interval, repeated every two revolutions after the completion of measurements. Initial state vectors in the inertial reference frame, solar pressure coefficients and empirical perturbations are solved for together with station biases. Thus, on average, a new solution is obtained once per day. Hence, for any time there are 7-9 different solutions for each SV. They were used to get the improved ephemeris data by averaging them and applying a filtering procedure with a 2-RMS criterion. In this way, orbits of 3 GLONASS satellites (69, 79, 71) have been computed covering a 3-month time span since the beginning of 1999. Finally, their positions have been obtained with a 30-minute time step for the same points as the broadcast orbits.

Actually only the initial state vectors and final values of EOP are stored in the data base (DB). So any propagation of the stored state vectors leads to orbits different from the transmitted broadcast ones. Such orbits in particular have been used for the determination of the transformation in (Mitrikas et al., 1998). At the moment only those data can be used for the long-term monitoring of PZ-90 GLONASS. So in order to understand whether the result obtained in the earlier work was influenced by possible orbit

uncertainties, it was decided to compare the transformation parameters based on actually transmitted and post-processed ephemerides.

The distributed GLONASS ephemerides are affected mainly by prediction errors. The influence of the EOP propagation is not critical except in some cases where LOD is too rough. In most cases, prediction error is in the along-track direction, and hence it can be reduced by applying so-called frequency-time corrections to the on-board clocks. The change in the prediction error can be considered as a random process in which the RMS error grows with time of prediction. In the case of the post-processed orbit, random variations are smaller because here there is no prediction interval and 7-9 different solutions are averaged for each point. But indeed here perhaps we have larger uncertainties because in the real OD process, the EOP are not updated every day. This is especially important for the UT1-UTC correction because its propagation error can be large. This error is reflected in the post-processed ephemeris data and hence in the transformation parameters. Consequently, it was expected that variation of rotation around the Z-axis should be less for the broadcast data.

The implementation of PZ-90 GLONASS reference frame is partially described in (Mitrikas et al., 1998). Here it will be repeated only that the regular facilities network consists of 4 stations: Moscow, St. Petersburg, Eniseisk and Komsomolsk. The transmitted GLONASS ephemeris data are to be represented in this conventional terrestrial reference frame. But because of errors in the PM values used, the reference frame set up by the ephemeris is not stable relative to any Earth-fixed reference frame.

Thus for the determination of the transformation parameters, two sets of orbits in PZ-90 GLONASS have been prepared:

- Broadcast transmitted positions of 8 satellites for the complete IGEX-98 period
- Post-processed positions of 3 satellites from different planes for the period from January 1999 until April 1999.

Transformation Parameters Determination Procedure

The Least Squares Method (LSM) was used to get Helmert parameters. The method of determination and SW have been developed in the frame of work sponsored by RSA in 1996-97. It was the initial intention to use the same programs as in (Mitrikas et al., 1998) with the aim to compare new and old results. Three complete iterations were performed for every determination to efficiently exclude all suspicious data using a 2.5-RMS criterion. State vectors in ITRF94 were treated as measurements and transformed PZ-90 GLONASS vectors were considered as their calculated values.

As was already mentioned, generally transformation parameters were estimated from two different sets of orbit positions in PZ-90 GLONASS: broadcast ephemeris collected in IGEX and averaged orbits based on data from SCC. Slightly different scheme of determination has been applied to these data sets.

The transformation parameters based on the transmitted broadcast data have been determined for the whole 6-month IGEX period. In order to estimate the accuracy and the impact of orbit modeling, basically 4 different series have been calculated. Three of them were related to different orbit planes and one series involved all data. One additional series of solutions without rejection of suspicious data was prepared for the evaluation of the effect of data filtering. All the periods where the MCC orbits seemed not to be very good have been excluded from consideration. In particular, this caused the exclusion of all data from March 1999 related to the second plane. Moreover, only two satellites in this plane were tracked by the laser network instead of three as in each of the two other planes. Thus, the total weight of the second plane in the common solution is approximately half that of the first or the third plane. A single determination involved 16 days of data normally corresponding to about 750 positions of each satellite at a 30-minute time step. The solutions were performed at an 8-day step to provide the dependency of the transformation on time. The beginning of the first solution was set to the beginning of the first orbit adjusted in the MCC. Thus, each solution covered exactly two consecutive laser-based orbit arcs.

The scheme used in (Mitrikas et al., 1998) was repeated for the averaged ephemeris processing. Since the source of the ephemeris was the same, this approach allowed direct comparison of the new and old results. Here PZ-90 GLONASS positions of only 3 satellites from different planes were available. They were processed separately and together. Each solution covered 20 days and the step between the solutions was 2 weeks.

As was expected, about 98% of the data were actually used. That is why there is not any visible difference between the results with or without data rejection. The LSM weighting, as in the previous work, assumed 1 m error in the radial direction and 5 m in along- and cross-track. It is important that the same SW was used for the determination of parameters in this work and in (Mitrikas et al., 1998). This was done especially to exclude possible influence of the SW bugs on the result because X and Y shifts adjusted in 1997 still have not been explained.

Although the transformation was confirmed to be time-dependent, the averaged common solutions for the 6-month IGEX period were used to calculate the transformation from PZ-90 GLONASS to ITRF94. This included coordinate data of all 8 GLONASS satellites tracked by the laser network. Their positions in PZ-90 GLONASS and ITRF94 were represented by the MCC orbits and transmitted ephemeris, respectively.

$$\begin{bmatrix} x \\ y \\ z \end{bmatrix}_{ITRF94} = \begin{bmatrix} -0.03 \text{ m} \\ 0.02 \text{ m} \\ -0.38 \text{ m} \end{bmatrix} + (1 + 9 \times 10^{-9}) \begin{bmatrix} 1 & -1.713 \times 10^{-6} & -0.060 \times 10^{-6} \\ 1.713 \times 10^{-6} & 1 & 0.192 \times 10^{-6} \\ 0.060 \times 10^{-6} & -0.192 \times 10^{-6} & 1 \end{bmatrix} \begin{bmatrix} u \\ v \\ w \end{bmatrix}_{PZ-90GL}$$

In order to analyze the result, the transformation determined in (Mitrikas et al., 1998) is also included here. Note that the parameters below have been obtained as a result of 20-months' processing from November 1995 to June 1997. Coordinates of two satellites in PZ-90 GLONASS were calculated by averaging SCC data, and the positions in ITRF were determined in GEOZUP Company with the same SW used in this work.

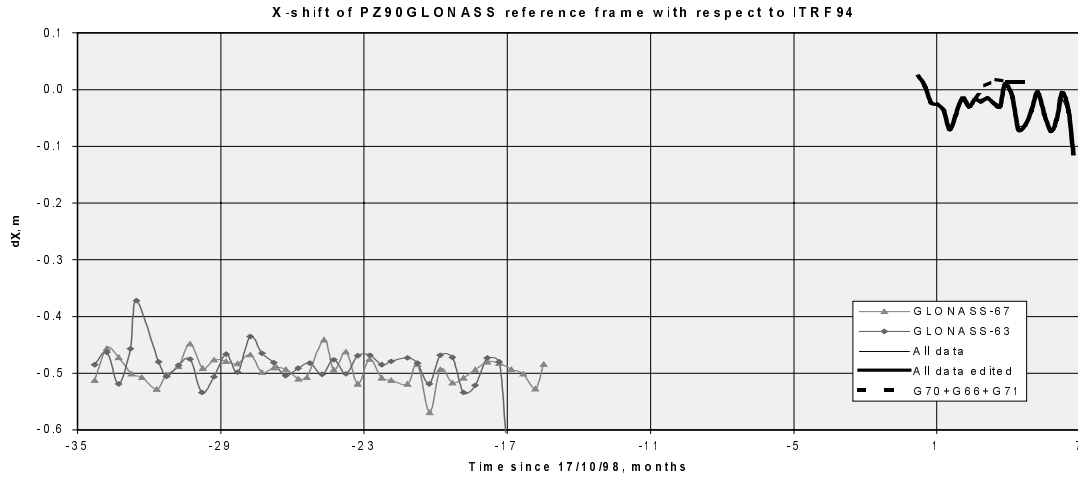


Figure 1.

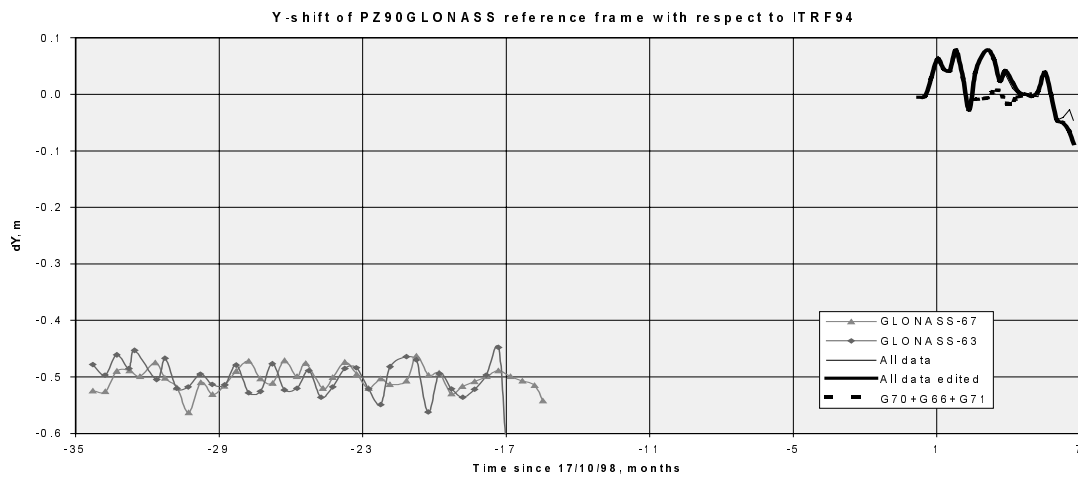


Figure 2.

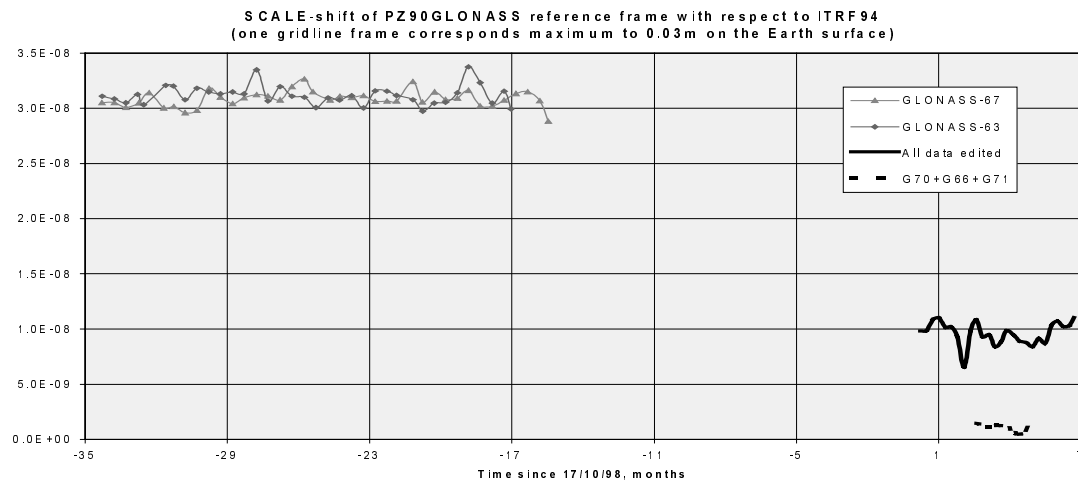


Figure 3.

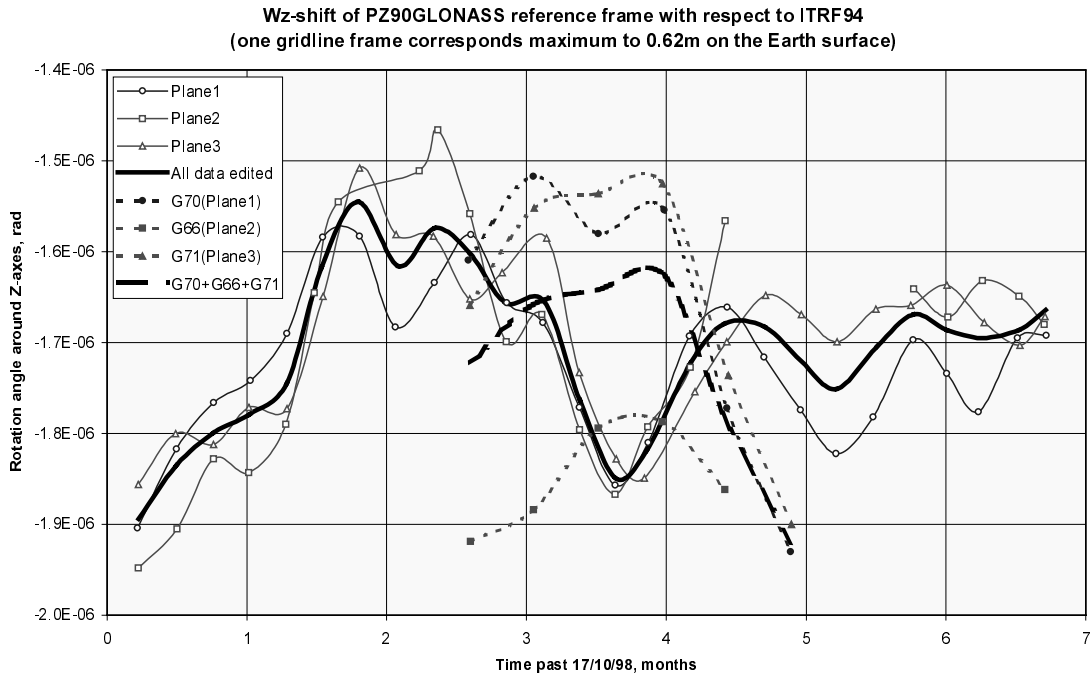


Figure 4.

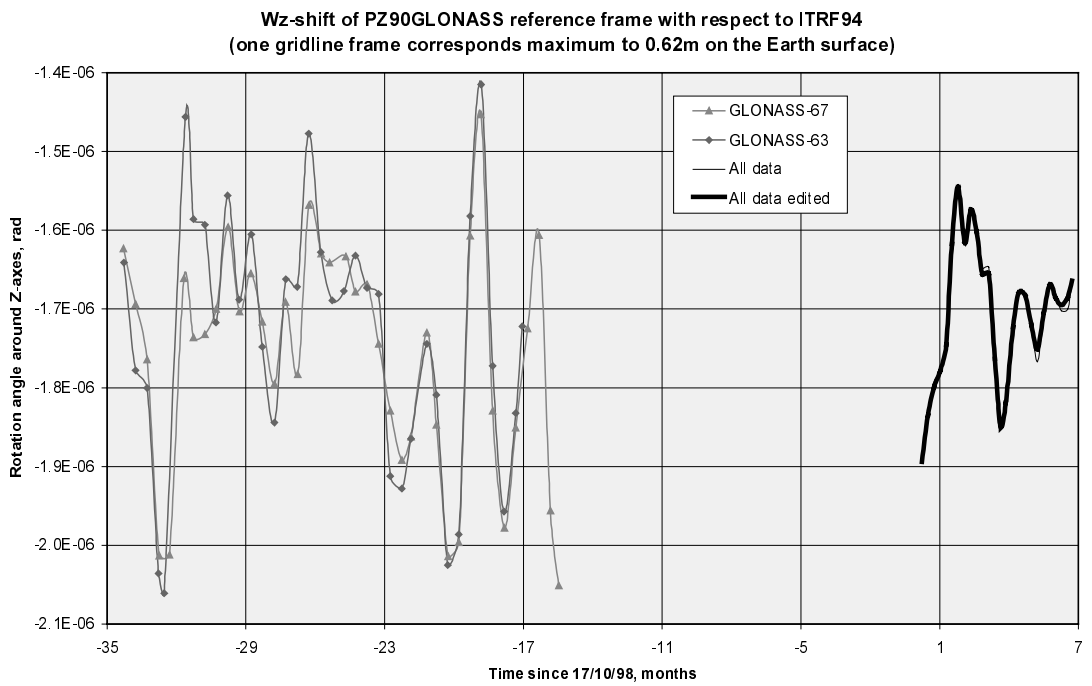


Figure 5.

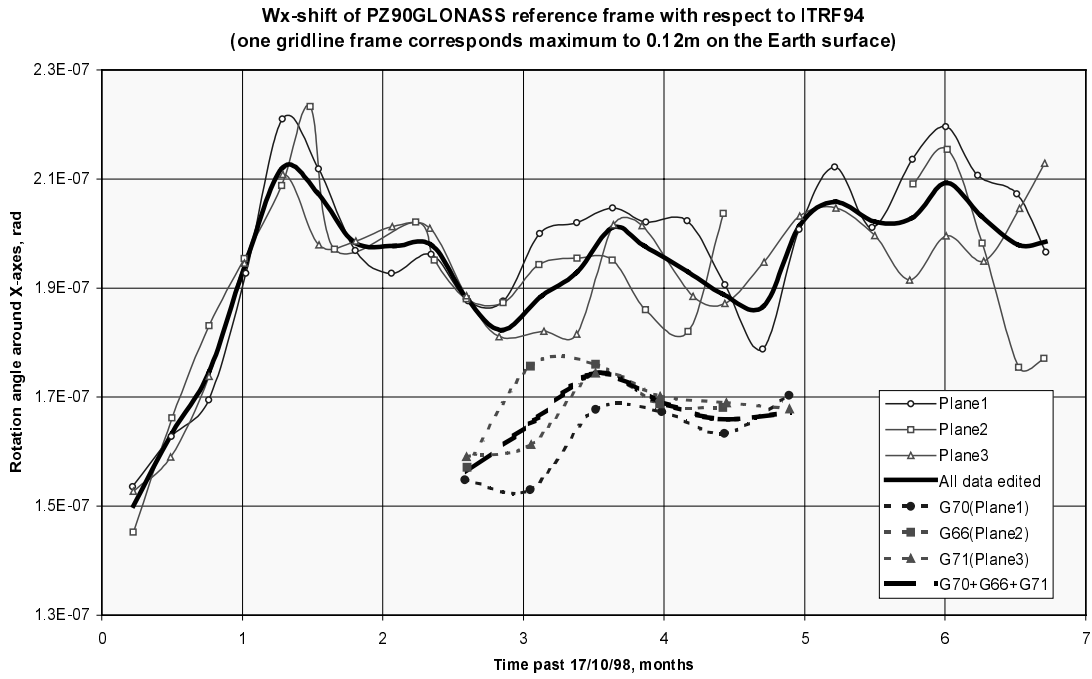


Figure 6.

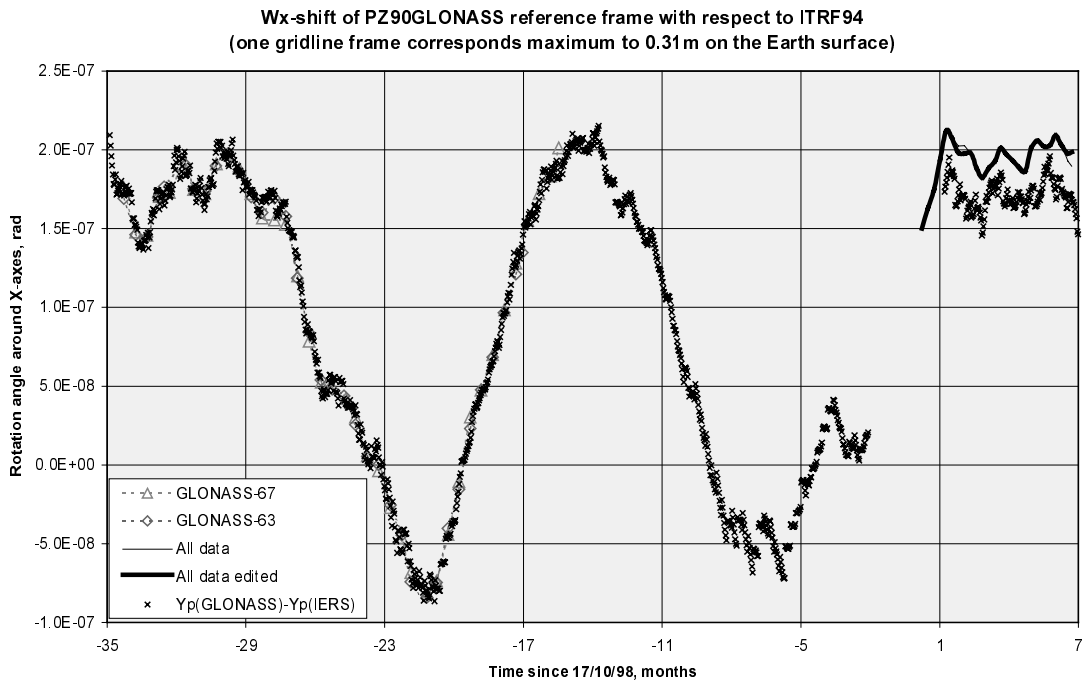


Figure 7.

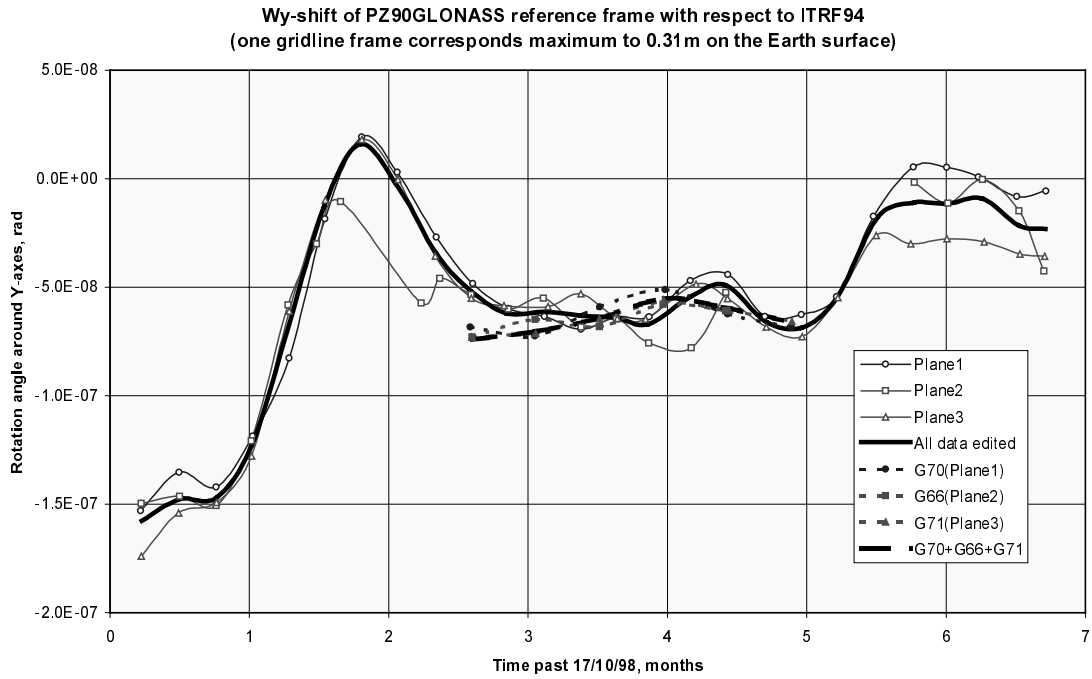


Figure 8.

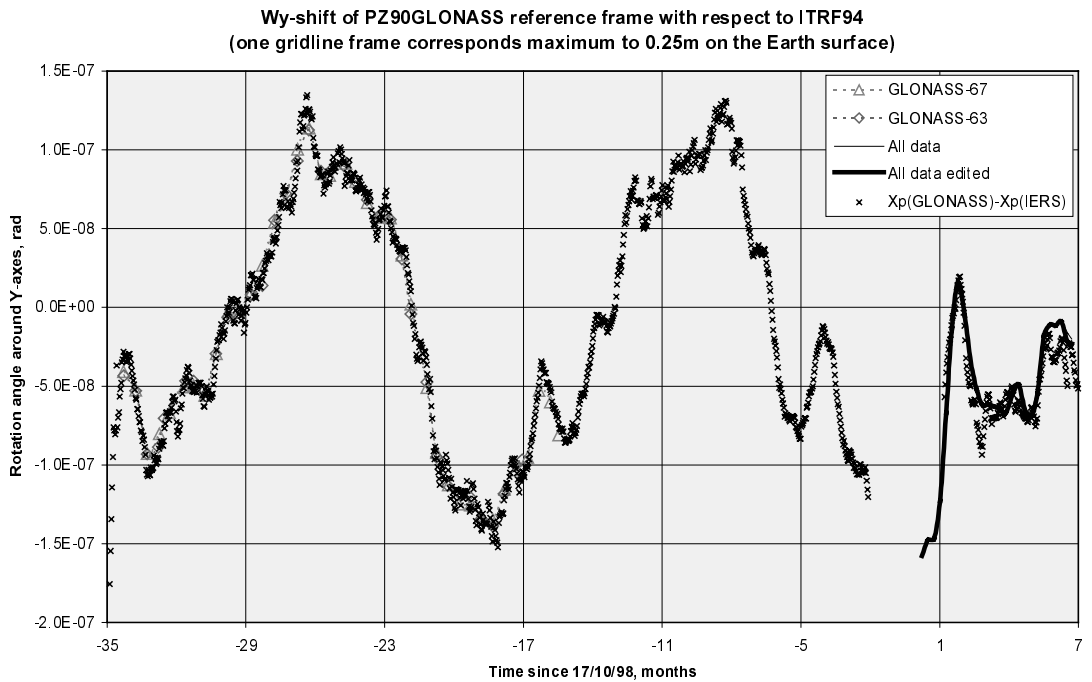


Figure 9.

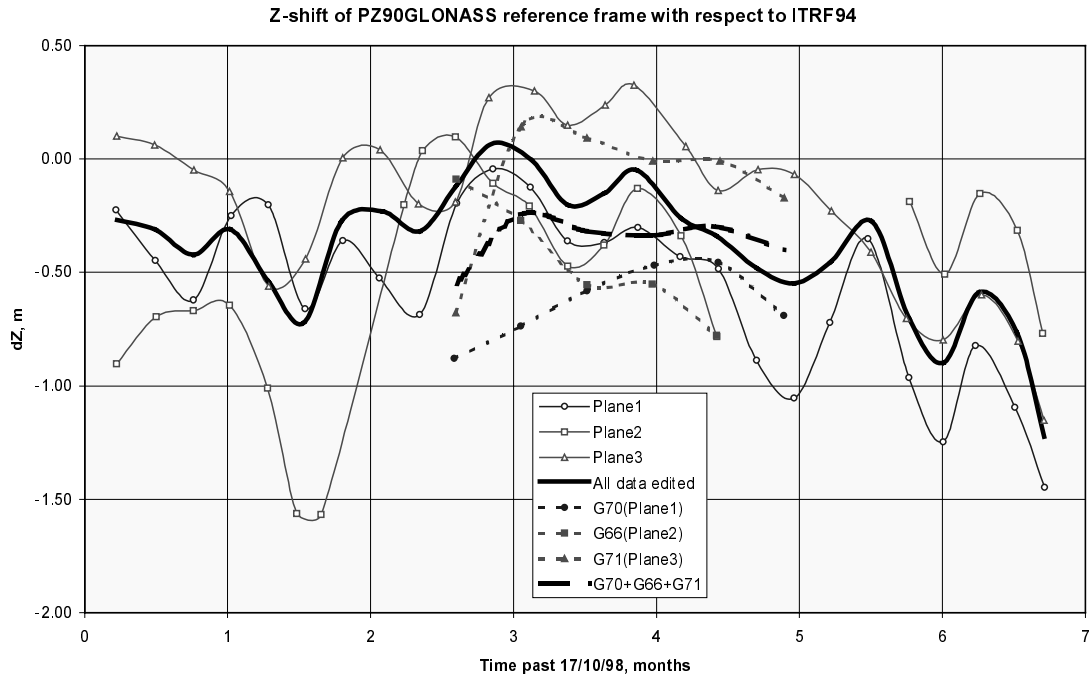


Figure 10.

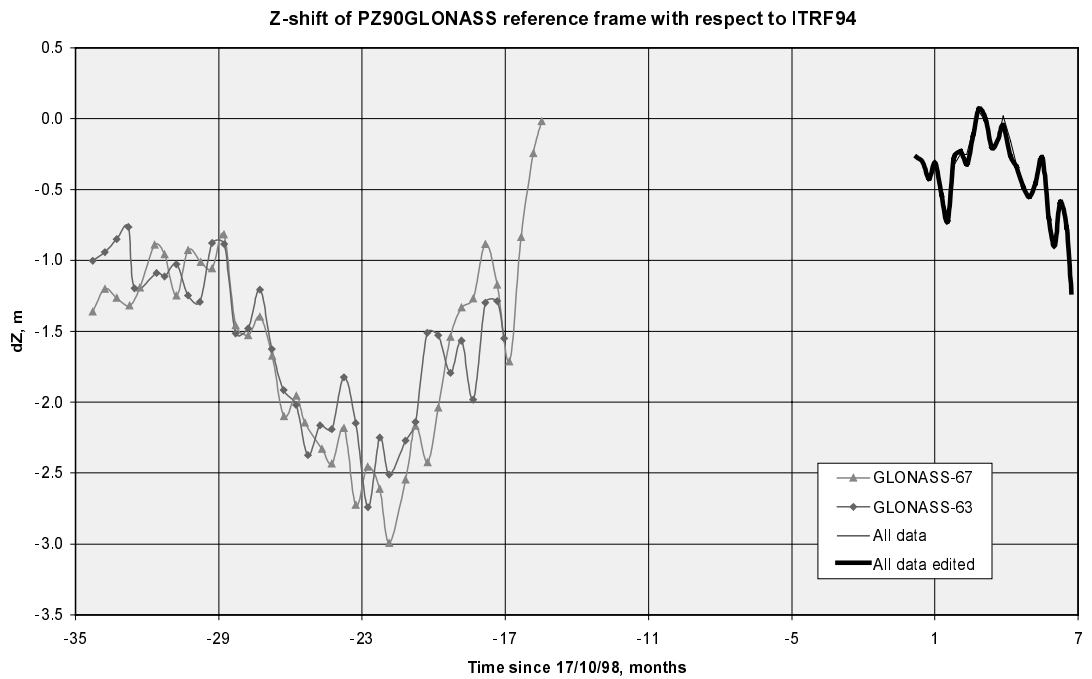


Figure 11.

$$\begin{bmatrix} x \\ y \\ z \end{bmatrix}_{ITRF94} = \begin{bmatrix} -0.49 \text{ m} \\ -0.50 \text{ m} \\ -1.57 \text{ m} \end{bmatrix} + (1 + 31 \times 10^{-9}) \begin{bmatrix} 1 & -1.745 \times 10^{-6} & -0.020 \times 10^{-6} \\ 1.745 \times 10^{-6} & 1 & 0.091 \times 10^{-6} \\ 0.020 \times 10^{-6} & -0.091 \times 10^{-6} & 1 \end{bmatrix} \begin{bmatrix} u \\ v \\ w \end{bmatrix}_{PZ-90GL}$$

For the analysis of results, plots are presented in figures 1-11. Part of them shows IGEX results only and the other part includes the parameters determined from GLONASS-63, 67 data in (Mitrikas et al., 1998). Here all the series based on IGEX data are plotted with solid lines and the series derived from post-processed ephemerides are shown with dashed lines. The series involving all available reliable data are labeled ‘all data edited’ and ‘G70+G66+G71’, correspondingly.

Transformation Parameters Analysis

Previous investigations postulated that transformation from PZ-90 GLONASS is affected by some time-dependent fluctuations. Most of them have a periodic character with more than a one-year period. Therefore, in order to find the average values of the transformation parameters it is necessary to monitor them for a long time period. From this perspective, the results reported at ION-98, covering 20 months, seem to be very important. Thus, the analysis of the transformation involves those data as well in order to get reliable conclusions. According to (Mitrikas et al., 1998), three parameters - translation of the origin along X and Y axes, and scale - showed very good stability. The remaining four - translation along Z-axis and all rotations - were unstable with probably periodic variations.

Translations Along X and Y Axes

Variations of the origin are limited to ± 5 cm around their average values (Figures 1,2). However, the Y-shift shows some downward slant. In fact such a change is not critical due to its value of 5-10 cm for half a year. Certainly both components can be considered as zeros. What is still not clear is half a meter difference in the results obtained in (Mitrikas et al., 1998) and in this work. It must be noted there is no difference between the solutions based on the transmitted ephemeris and the averaged SCC data. The only source of the non-zero translations determined in (Mitrikas et al., 1998) can be SCC data because the SW used for orbit determination on the laser data and for the transformation determination has not been changed so far. It is very difficult even to imagine the source of such translation. The reference frame PZ-90 GLONASS is represented by station coordinates which have been adjusted from two-way range measurements. Since the tracking data were distributed nearly evenly, there is no reason for the translation of the origin in the equatorial plane. In fact, for calculation of the positions of GLONASS satellites in the PZ-90 reference frame, a special program was written in SCC in the frame of (Mitrikas et al., 1998). At the moment there is no information as to exactly which program was used to prepare SCC data for this work. But the following reason seems to be possible: in the SCC data preparation the wrong rounding function has been used in the past. As a result, all the coordinates in PZ-90 GLONASS were increased by an average of 0.5 m. Two ideas confirm this assumption. First, the formats of data

obtained from SCC are different. Now all data are represented as real values instead of integer values as was the case before. The second reason is the behavior of the Z-translation (Figure 11) discussed below. Even a short look at the plot raises the question: Why is the new curve higher than the old one? This unexpected difference is about 0.5 m with the same sign as for X- and Y-translations, so probably the shift of the origin as reported in (Mitrikas et al., 1998) must be increased by 0.5 m in all coordinates.

Scale

A similar picture can be observed for the scale parameter. Its behavior is even stranger. The determined values are 31 ppb (about 20 cm at the Earth's surface) in (Mitrikas et al., 1998), 9 ppb (6 cm) from the broadcast data and 1 ppb (1 cm) from the averaged SCC data. It should be mentioned that orbit positions in ITRF always were related to the satellite center of mass. According to the ICD, the broadcast ephemeris is referenced to the navigation antenna phase center. But there is a clear difference of 1.6 m between these two points. Due to circular orbits and since it is concentrated in radial direction it must be recalculated in the scale parameter which shows in what degree all points in one reference frame are farther or closer to the origin than in another one. So the expected value was 63 ppb. In practice there is nothing similar (Figure 3). Probably SCC data related to GLONASS-66, 70, 71 are referred to center of mass, but the scale obtained in (Mitrikas et al., 1998) from GLONASS-63 and -67 data is completely unexplained. There are two hypotheses about the scale derived from the broadcast ephemeris. There seems to be a mistake in the recalculations to the antenna phase center. Nevertheless there is also a possible systematic prediction error in the radial direction.

All other parameters basically confirm the result from (Mitrikas et al., 1998). All they are still affected by periodic variations.

Rotation About Z-Axis

This is the most valuable part of the transformation. Z-rotation is very highly correlated with the UT1-UTC correction. Normally the UT1 correction is updated once per week in the regular SW. Actually absolute UT1 error makes no sense for the accuracy of orbit determination unless such error reaches critical values of several seconds. This fact is well known and it takes place because satellite orbits are sensitive to UT1-UTC through third body only. Any error in the UT1 correction is compensated by orbit node and finally orbit has normal orientation with respect to the terrestrial reference frame where tracking stations are located. However, if the UT1-UTC error has some drift, it is reflected in the orbit accuracy. So the critical parameter is LOD. Theoretically, it has no error just after UT1-UTC difference updating and maximum error just before. So generally accuracy of the transmitted ephemeris should degrade slowly during a week and then after EOP updating it becomes better at the moment. The value of LOD error depends on the methods and algorithms used for the prediction of UT1-UTC, but hopefully it has no systematic components. Thus, the broadcast ephemerides are not affected strongly by the error in UT1-UTC prediction.

In fact, the SCC DB contains only final values of EOP. For this work, as in the previous work (Mitrikas et al., 1998), the predictions of satellite movement have been calculated from the initial state vectors stored in the DB after every regular OD. So all the a posteriori data calculated in SCC are based on the final EOP values. Indeed partially predicted EOP have been used in the real OD. The size of the predicted part was variable due to the reasons described above. Thus all satellite positions prepared in SCC PZ90 GLONASS system have absorbed errors of UT1-UTC prediction. Since those errors have no long period biases, the transformation error in the rotation around the Z-axis should decrease with an increase in the averaging time period. The total period processed in (Mitrikas et al., 1998) covered 20 months, so the average value obtained in that work is probably accurate enough.

It was expected that the transformation based on the broadcast ephemeris would lead to the same result in Z-rotation but with low fluctuations. Basically this work has confirmed such assumptions. The plot in Figure 5 shows the behavior of the 20-days Wz parameter determined in (Mitrikas et al., 1998) with the average 16-days Wz based on broadcast data. Obviously the IGEX period is not sufficient to get the exact value of the angle but clearly both results vary around the average of $-1.70 \cdot 10^{-6}$ to $-1.75 \cdot 10^{-6}$. The rotation parameters Wz derived from the separate processing of different planes are in very good agreement (Figure 4). However the curve based on SCC data of GLONASS-66 seems to be affected by constant systematic error. This fact has no any reasonable explanation. The broadcast ephemeris data for the second plane include only two satellites (GLONASS-66, 79) and the respective Wz coincides with other data. Anyway, probably the average of the old and new results ($-1,73 \cdot 10^{-6}$) is accurate enough. Any improvement of the result makes no sense since the fluctuations of the Wz rotation exceed $0.15 \cdot 10^{-6}$ (about 1 m along the equator) from the average.

Rotations About X- and Y-Axes

Both parameters are absolutely correlated with the errors in GLONASS polar motion. This fact and its reasons are explained in detail in (Mitrikas et al., 1998). To avoid the influence of PM errors in that work, all the data in PZ90 GLONASS have been recalculated with IERS PM instead of using the values from SCC. As a result, both rotations became negligible. It has been concluded that there are no rotations around X and Y axes between PZ90 GLONASS set up by regular station coordinates and ITRF.

The new results based on SCC data are very similar. When the broadcast ephemerides were calculated, the predicted values of PM were used. So the larger fluctuations of corresponding transformation parameters were expected. The results are presented in Figures 6 and 8. Generally the assumptions have been confirmed, but there is some systematic bias between the data based on broadcast and post-processed SCC data (Figures 7, 9). The only difference is the use of final or predicted polar motion. Looking at the plots one can conclude that prediction of the Xp component has no visible errors but there is a bias of 5 ms of arc in the prediction of the Yp component. Actually SCC PM is predicted taking into account a very long history of values (Bykhanov, 1996). So maybe such error is caused by the curve of the Yp component. In this case, short-term

biases may occur for both components at different time periods. However the stability of the bias during the whole IGEX looks strange. The available information does not make it possible to draw a final conclusion. Unlike the Wz rotation, here it is necessary to separate between PZ90 GLONASS reference frames specified by ephemeris and by station coordinates. For the frame set by tracking facilities, both rotations Wx and Wy should be considered as zero. Taking the above-mentioned bias into account, perhaps it is possible to speak about the Wx rotation of $0.25 \cdot 10^{-7}$ rad. But indeed such a reference frame would be of interest to users only if SCC used IERS PM. Thus, for the determination of the average Wx and Wy rotations, the plot of the error between GLONASS and IERS polar motion can be used (Figures 7, 9). From it the following values can be proposed: $W_x = 0.08 \cdot 10^{-6}$, $W_y = 0.01 \cdot 10^{-8}$. Basically there is no need in any measurements for their long-term monitoring; it is just enough to have the used values of PM.

Z-shift of the Origin

This is the most critical question at the moment. Translation of the origin along Z-axis varies much depending on the data involved. The main reason for such fluctuations maybe the very limited network of regular stations and insufficient number of measurements. It must be noted that all regular facilities are located between 50 and 60 degrees North latitude. Relatively high inclination, empirical solar pressure parameters and different tracking data sets for different satellites perhaps are the reasons for the errors in the Z-shift of orbits. Nevertheless, all the processed data show similar results. It is especially important that there is nearly no difference between the results based on broadcast and post-processed ephemeris (Figure 10). This allows the analysis of Z-translation over the long time period from November 1995 (Figure 11). Unfortunately, a quite long and extremely important time period is missed. However the correlation between Z-translation and the error in GLONASS PM in Yp has been detected in (Mitrikas et al., 1998). It is not so evident from IGEX results, but in general, the period of Z-translation fluctuations should coincide with the period of the Wx and Wy rotations because all the problems are caused by the same methods and algorithms used in the regular OD. As was mentioned in (Mitrikas et al., 1998), probably all the errors derive from old precession and especially nutation models. In the analysis of X and Y translations, the hypothesis has been proposed that all the positions of GLONASS-63 and 67 were computed in SCC with random rounding error varying from 0 to +1 m with 0.5 mathematical expectation. Such an error could not cause any systematic biases except the shift of the origin. With this assumption the correlation between Z-translation and Yp error becomes visible again. Looking at Figure 7 the behavior of the Z-translation for the missed period can be assumed. The averaged value of the Z-translation can be adopted as much as -1.1 m. Indeed this value is perhaps not as accurate as other transformation parameters. That is why additional monitoring is required to define it more precisely. Because of the assumed correlation with the Yp error, the value of the Z-shift free of PM errors may be different. The reason for the correlation is described in (Mitrikas et al., 1998), and its estimated influence is about -40 cm. So the expected value for the transformation from the tracking facilities reference frame is -1.5 m.

Simplified GLONASS Solar Pressure Model

The developed solar pressure model is complicated enough. Moreover due to necessity to include empirical acceleration the question arises whether it is really so important to model all the parts of the satellite design. That is why in the frame of GLONASS laser data processing in 1996-97 the idea came to prepare some simplified model for all GLONASS satellites. Such an approach seems to be similar to that used for GPS satellites for which solar radiation pressure models are now included as a part of IERS standards. Of course it is difficult to build a very precise model on the basis of laser measurements only but they could be used as the first approximation to be adjusted later from phase data. Additionally there was a hope that, properly determined, such a model could absorb part of the empirical acceleration influence. Such work was actually done in 1997 but it was only described in an internal GEOZUP technical report with extremely limited distribution. There were four main stages to get the final solution:

- Preparation of the data consisting of the perturbation accelerations due to solar pressure and empirical forces.
- Determination of those parts of orbits where the prepared data do not show any irregular behavior.
- Simplified formula choice.
- Determination with LSM of the coefficients and comparison with the results from the complete model.

To avoid the unmodeled influence of solar panel orientation on the eclipse orbit arcs, only non-shadow periods have been taken into account. In the preparation stage, the set of data has been combined from orbit positions and accelerations at a 15-minute time step. The choice of the expression for the simplified model was perhaps the most difficult problem. Basically the satellite supports three-axis orientation holding the sun in the fixed plane relative to the bus. The solar pressure accelerations are supposed to be symmetric with respect to the body fixed reference frame. Mainly the value of solar pressure in the body-fixed reference frame depends on the angle between the direction to the sun and X-axis of the spacecraft. Therefore the initial formula for the investigations had the following form:

$$A = \sum_1^n a_n \sin n\alpha + b_n \cos n\alpha$$

where α is the mentioned angle, a_n and b_n are the coefficients to be solved for.

As a result of the investigations performed for both satellites, the following conclusions have been formulated:

- The LSM residuals actually are almost independent of the number of terms in the expression above.
- The result becomes stable enough on the long arcs only.
- The parameters of simplified models determined separately for different satellites coincide well on the periods from half a year.

- The initial set of data should be carefully filtered in order to obtain a reliable result.

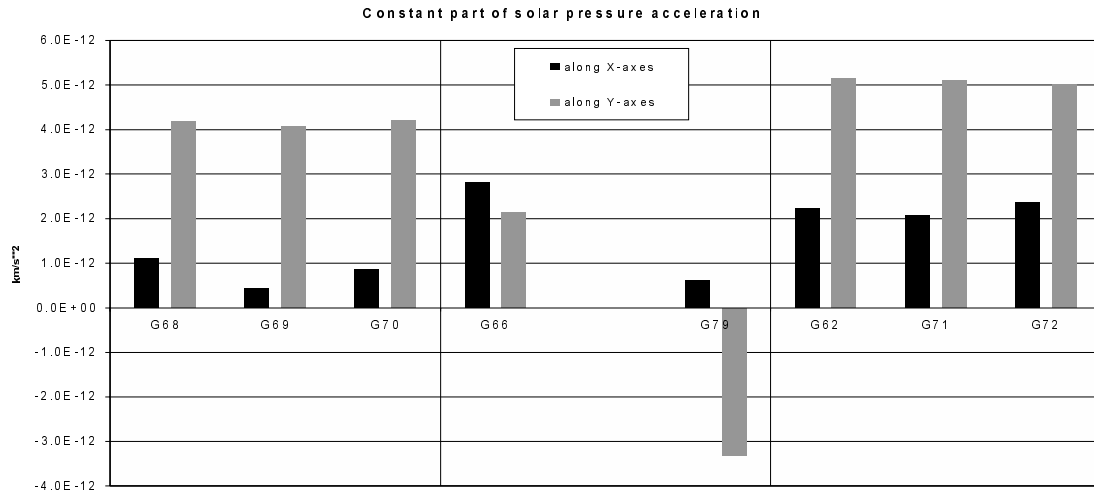


Figure 12.

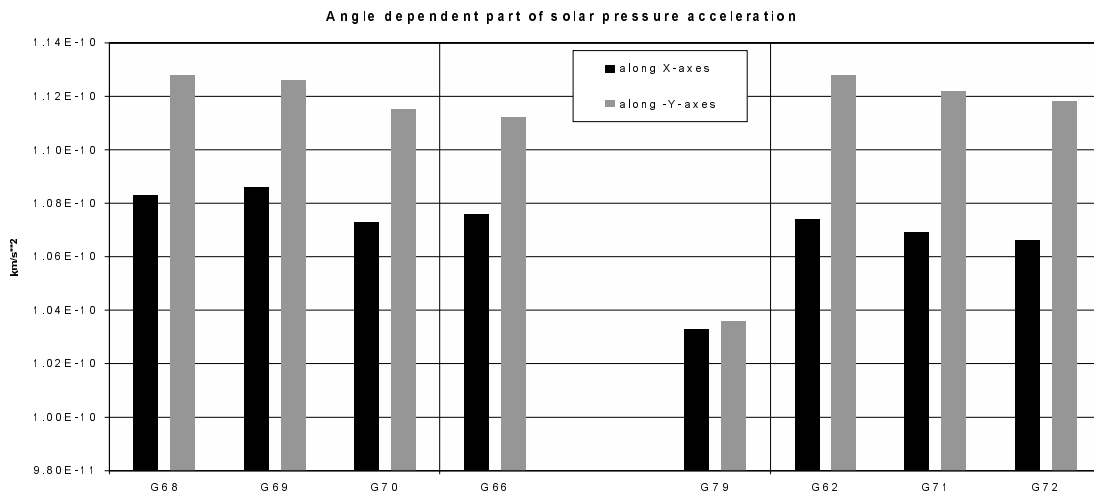


Figure 13.

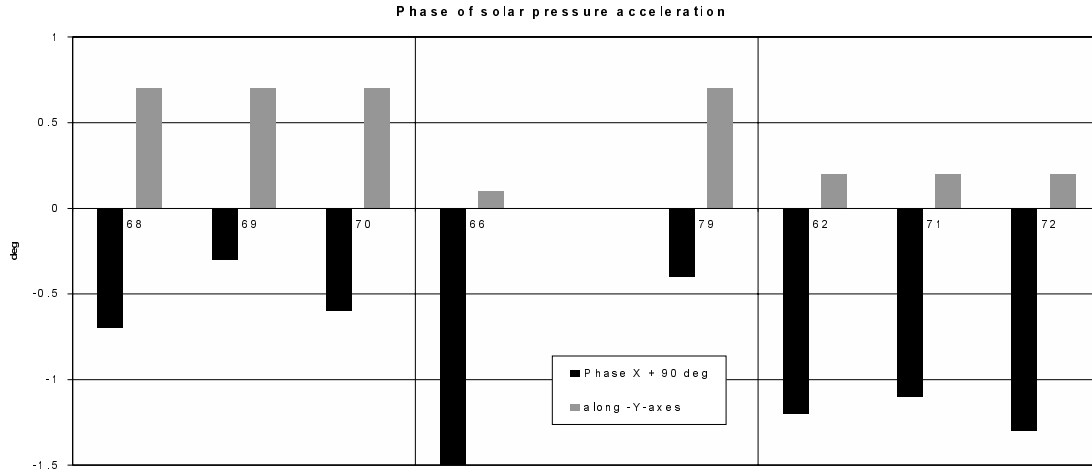


Figure 14.

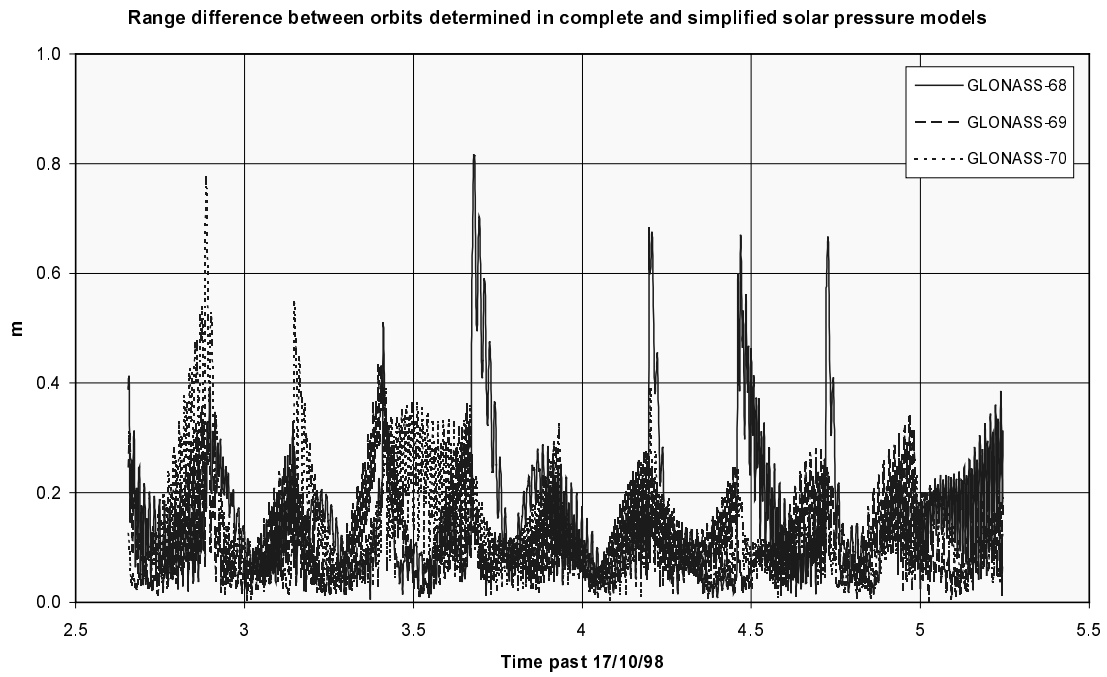


Figure 15.

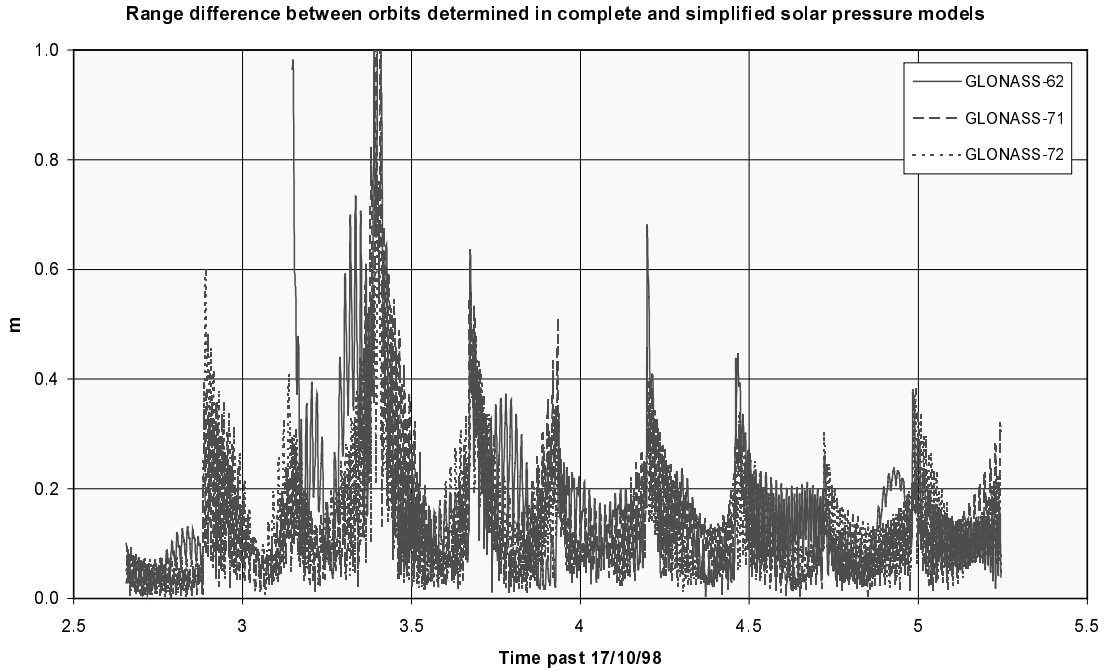


Figure 16.

Hence it was decided to adjust 3 parameters for both X and Y components of the acceleration in the body-fixed reference frame because the inclusion of terms with 2α , 3α , etc. did not affect the final residuals. That was not exactly true for the clear solar pressure force but the effect of high terms became negligible with the addition of the empirical accelerations. For simplicity the scaling effect A_c^2/R^2 has been included in the expression. Finally OD of both satellites with the simplified model has been repeated for a 6-month period for comparison with the precise orbits. The difference between those two orbits did not exceed 0.8 m for GLONASS-63 and 0.35 m for GLONASS-67 and in most cases, it was below 0.2 m.

When MCC orbits of 8 GLONASS satellites have been calculated the determination of the simplified solar pressure has become possible on the basis of IGEX laser data. The set of data as described above has been prepared for all satellites. For this purpose, all the solar pressure coefficients and the empirical accelerations were analyzed as time dependent series. From their comparison, only those parts of orbits have been retained where the plotted values did not raise any questions. Normally the problematic parts of orbits were close to the beginnings and the ends of shadowing. Mostly they have been explained by the solar panel orientation algorithm. Some additional fluctuations of the acceleration occurred for the eclipse orbits also, but the reason was probably related to accounting for empirical accelerations in the shadows. Moreover the accuracy of some arcs has been affected by operator errors described above in this paper. Anyway all the suspicious data have been excluded.

In order to check the consistency of the data, separate solutions have been performed for all satellites. Three adjusted components - constant part and the amplitude and phase of the acceleration - are presented in the plots in Figures 12-14. It can be easily detected that the behavior of GLONASS-79 differs much from others. Therefore it was removed from the merged set of data and the final coefficients were determined without its data. There is also some difference in the results from different planes. Currently this effect has no explanation. Finally, after 7 satellites' data have been merged, one additional common solution was obtained. It included almost 102,000 points or about 90% of the data filtered with a 2.5 RMS criterion.

OD of all 8 satellites has been carried out once again with this simplified model for a 3-month period for the validation of the coefficients presented below. Then these new orbits have been compared to those determined in the complete model. The resulting differences for two planes are presented in Figures 15-16. Where there were sufficient tracking data, the range difference between orbits hardly exceeds 30 cm. Taking into account the expected accuracy of 1 m of the precise orbits and relatively long 8.5 OD interval, it may be concluded that the simplified model can be used for GLONASS modeling.

$$A_x = A_e^2/R^2 \cdot (0.001 - 0.108 \cdot \text{Cos}(\alpha - 0.017)) \cdot 10^{-9}$$

$$A_y = A_e^2/R^2 \cdot (0.004 - 0.112 \cdot \text{Sin}(\alpha + 0.008)) \cdot 10^{-9}$$

$$A_z = 0$$

where A_e is an astronomical unit (149597870.66 km), R is the range of the heliocentric satellite vector.

Conclusions

IGEX has presented a unique chance to find the exact transformation from the PZ90 GLONASS reference frame to ITRF and WGS84. Despite the exclusive importance of the problem, no official parameters have been adopted yet for the common use of SNS GPS and GLONASS. Several investigations on this question have led to similar results, but the problem still remains actual because of the separate opinion of TSRMD, which is responsible for the PZ90 solution. IGEX should recommend at least preliminary values of the transformation parameters. Perhaps their values will be defined more precisely in future but even available values are enough for most users.

This work is one of several dedicated to the problem of transformation between GPS and GLONASS reference frames. It is important among others because it continues the investigations sponsored by RSA and reported at ION-98. Those results have covered nearly a 20-month time span and for the first time, the discussed transformation has been determined as time dependent. Its major fluctuations are quasi-periodical with a period of more than 1 year. Clearly 6 months of IGEX data are not enough to get average values. That is why the validation of old results and their comparison to the newly obtained IGEX data are very important for the preparation of standard transformation parameters.

Unlike in (Mitrikas et al., 1998), laser-based GLONASS orbits in ITRF have been prepared in MCC in the routine mode. This of course caused some additional problems with the orbit accuracy. Their reasons are mentioned in this paper. The positive effect of this work is that all the suspicious arcs have been recalculated in MCC. The new data related to last 3.5 IGEX months has already replaced those obtained earlier. Unfortunately at the moment they have become ready, there was no time to compute new transformation parameters until the IGEX meeting. Anyway the results are mostly affected by the orbit in PZ90 GLONASS errors so any significant errors are not expected.

It should be stated once again that the joint RSA and NASA decision on a GLONASS laser tracking campaign adopted in 1994 made possible the long term monitoring of the PZ90 GLONASS reference frame. Certainly it is very important to establish final values of the transformation parameters.

Several separate steps have been done towards the final results.

1. Gathering and processing of the laser data of 8 GLONASS satellites. Computation of their orbits in the ITRF94 reference frame. Here almost all the data collected from the whole laser network have been involved except for a few stations. The accuracy of the orbit depends on the satellite but in general the expected RMS is 1.5 m. This work was done by the MCC laser group. Then all the problematic orbit parts have been removed in order to avoid their influence on the results.
2. The broadcast positions of 8 GLONASS satellites have been computed from the ephemeris data collected by IGEX stations. The data have been prepared with a 30-minute time step to avoid any integration errors.
3. The averaged orbits in PZ90 GLONASS have been determined on the basis of information from regular SCC OD. For that purpose 7-9 positions from different solutions have been averaged for each point. A 3-month period of 3 GLONASS satellites was covered with 30-minutes time step.
4. Transformation parameters from PZ90 GLONASS to ITRF94 have been computed from the broadcast data and MCC orbits. That was done independently for different planes and merging all data together. For the evaluation of time dependency, a series of 16-day solutions have been performed with an 8-day step. Additionally one common solution from all data available has been prepared.
5. Transformation parameters from PZ90 GLONASS to ITRF94 have been computed from the averaged post-processed data and MCC orbits. The scheme of their determination has been taken from (Mitrikas et al., 1998). All 3 GLONASS satellites have been processed independently involving 20-days of data in each solution with a 2-week step between the solutions. Thus the prepared series may be considered as extensions of (Mitrikas et al., 1998). For

simplification of the comparison one common series with all 3 satellites merged has been calculated.

- The analysis of the obtained parameters was performed in order to determine the average values to be recommended as standard parameters. Generally the new data confirm the results from (Mitrikas et al., 1998). The major difference is related to the translation of the origin and scale. However with the hypothesis presented in this paper on rounding errors, the difference between the current result and (Mitrikas et al., 1998) does not exceed 20 cm. Probably this value may be considered as the expected accuracy of the proposed transformation. But even without 0.5 m correction of all the origin coordinates the difference does not seem to be critical because the variations of other parameters are obviously large in magnitude. The proposed transformation is presented below:

$$\begin{bmatrix} x \\ y \\ z \end{bmatrix}_{ITRF} = \begin{bmatrix} 0.0 \text{ m} \\ 0.0 \text{ m} \\ -1.1 \text{ m} \end{bmatrix} + (1+9 \times 10^{-9}) \begin{bmatrix} 1 & -1.73 \times 10^{-6} & -0.02 \times 10^{-6} \\ 1.73 \times 10^{-6} & 1 & 0.08 \times 10^{-6} \\ 0.02 \times 10^{-6} & -0.08 \times 10^{-6} & 1 \end{bmatrix} \begin{bmatrix} u \\ v \\ w \end{bmatrix}_{PZ-90GL}$$

- A simplified GLONASS solar radiation pressure model has been proposed. It was determined with the LSM method from the precise GLONASS MCC orbits. A special investigation to choose the formula led to the final expression. Orbits of all satellites have been recomputed to validate the model. The correctness of the proposed model has been confirmed by the comparison between orbits in the complete and simplified models. The proposed expression is presented in this paper. It must be mixed with the empirical accelerations for accurate orbit determination.

Recommendations

From the user point of view, the amplitude of the user position fluctuations due to instability of PZ90 GLONASS may exceed 1.5 m. Taking this fact into account, the average transformation parameters determined in this investigation may be recommended for recalculation of PZ90 GLONASS coordinates to ITRF. Hopefully the transformation presented above is not far from the truth. In fact the exact reason for the periodic variations is still not defined. Of course they are connected with the models used. But since we do not know the reasons, we cannot predict the transformation for sure. Hence at the moment we can only suppose future behavior of the parameters from the plots prepared. But nobody can guarantee the determined average values to be valid for years. Thus the PZ90 GLONASS-ITRF transformation should be monitored at least from time to time.

As a result of the previous investigation, it was recommended to use external PM in the regular SW. However such a decision is beyond the responsibility of the authors. The new results confirm a high correlation of the transformation with the errors in GLONASS EOP. But now the bias in the PM predictions is being suspected, so more frequent

updates of final EOP should be recommended. Moreover short prediction period could also reduce the variations of Wz rotation. However for the exclusion of most errors the revision of the regular SW should be done to make it consistent with IERS models. Such an activity has already been initiated, so probably at some time in the future, the transformation will be stable. The next step on the way is to adjust the regular station positions to ITRF to transmit the broadcast data in this frame, similar to what was done by NIMA for WGS84 (NIMA, 1997).

Acknowledgements

Authors are very thankful to Mr. James A. Slater for his help in general editing of the paper.

References

- Bazlov, Y.A., V.F. Galazin, B.L. Kaplan, V.G. Maksimov, V.P. Rogozin (1999). GLONASS to GPS – A New Coordinate Transformation, *GPS World*, Vol. 10, No. 1, pp. 54-58.
- Bykhanov, E. V. (1996). Earth Orientations Parameters Determination Using Ranging of GLONASS Satellite, *Space geodesy and modern geodynamics*, IARAS, Moscow, pp. 60-90.
- Galazin, V.F., V.G. Maksimov, Y.A. Bazlov, B.L. Kaplan (1997). The Common Use of GPS and GLONASS: Accuracy Estimation of the Different Methods Used in the Determination of Transformation between PZ90 and WGS84, *Proceedings The International Radionavigation Conference*, Moscow, June 1997.
- GEOZUP (1996a). The Development of GLONASS Ballistic Model on the Results of Laser Tracking Campaign. *Scientific report in Russian*.
- GEOZUP (1996b). Determination of Conventional Terrestrial Reference Frame on 4-Years Period Using Geodetic Satellites Data. *Scientific report in Russian*.
- GEOZUP (1997). The Development of GLONASS Ballistic Model and Simplified Solar Pressure Model on the Results of Laser Tracking Campaign. 2nd edition. *Scientific report in Russian*.
- Glotov, V., M. Zinkovski, V. Mitrikas (1999). GLONASS Precise Orbits as a Result of IGEX-98 Laser Tracking Campaign, *Proceedings IGEX-98 Workshop*, Nashville, Sept. 13-14, 1999, JPL.
- Malys, S., J.A. Slater (1994). Maintenance and Enhancement of the World Geodetic System 1984, *Proceedings ION GPS-94*, Salt Lake City, Sept. 20-23, 1994, Inst. of Navigation.

- Merckulov, Y.A. (1997). The Questions of GLONASS Control, Responsibility and Foundation Including International Cooperation and Government Plans, *Proceedings The International Radionavigation Conference*, Moscow, June 1997.
- Misra, P., R. Abbot, E. Gaposchkin (1996). Integrated Use of GPS and GLONASS: Transformation between WGS 84 and PZ-90, *Proceedings ION GPS-96*, Kansas City, Sept. 17-20, 1996, pp.307-314, Inst. of Navigation.
- Mitrikas, V.V., S.G. Revnivkykh, E.V. Bykhanov (1998). WGS 84/PZ 90 Transformation Parameters Determination Based on Laser and Ephemerides Long-Term GLONASS Orbital Data Processing, *Proceedings ION GPS-98*, Nashville, Sept. 15-18, 1998, Inst. of Navigation.
- NIMA (1997). Department of Defense World Geodetic System 1984, Its Definition and Relationships with Local Geodetic Systems, *National Imagery and Mapping Agency Technical Report TR 8350.2*, Third edition, 4 July 1997.
- Rosbach, U., H. Habrich, N. Zarraoa (1996). Transformation Parameters Between PZ-90 and WGS84, *Proceedings ION GPS-96*, Kansas City, Sept. 17-20, 1996, pp. 279-285, Inst. of Navigation.
- Seidelmann, P.K. (1992). *Explanatory Supplement to The Astronomical Almanac*, P.K. Seidelmann, Ed., University Science Books, Mill Valley, California.

PZ-90 / WGS 84 Transformation Parameters Directly From GLONASS Range Measurements

Udo Rossbach

IfEN GmbH

Hauptstrasse 37, D-85579 Neubiberg, Germany

Abstract

Undoubtedly, the combined use of GPS and GLONASS brings along a number of advantages as compared to the use of either of the systems alone. However, GPS and GLONASS employ different coordinate frames to express satellite positions at a given time. To make full use of the combination, the transformation between these two frames must be known with sufficient accuracy.

Until recently, however, the determination of this coordinate transformation was obstructed by the non-availability of known sites surveyed in PZ-90 and/or by the limited number of available GLONASS receivers. In the IGEX-98 campaign, for the first time a significant number of GLONASS receivers were operated simultaneously at observation sites all around the globe.

The parameters of the coordinate transformation between PZ-90 and WGS 84 are conventionally determined by surveying sites in both coordinate frames and then comparing their coordinates. These sites can be located on the surface of the Earth (receiver locations) or in space (satellite locations).

This paper introduces a new method of determining the transformation parameters. Instead of surveying locations with known WGS 84 coordinates in the PZ-90 frame and comparing these coordinates, the transformation parameters are estimated directly from range measurements to GLONASS satellites at known WGS 84 observation sites.

The derived transformation parameters are presented and compared to other estimations.

Introduction

Many users of the GPS system, both in navigation and geodesy, meanwhile recognize the advantages of combining GPS with GLONASS satellite observations: The increase in the number of available satellites improves the accuracy of the positioning determination by improving the geometry of the tracked satellites. In mountainous or urban areas with parts of the sky blocked, only the additional satellite observations may make a position fix possible at all. Including observations to a different, independent satellite system will also improve the integrity of the navigation system. This is especially important for the use of GPS in aviation and other safety critical applications. For geodetic applications with their needs for high precision, the addition of GLONASS satellites may result in a faster and more reliable fixing of the integer ambiguities.

The coordinate reference frames used by GPS and GLONASS, however, are different. GPS employs the WGS 84 frame, whereas GLONASS makes use of a frame called Parametry Zemli (Parameters of the Earth) 1990 (PZ-90, sometimes also referred to as PE-90). Combining GPS and GLONASS in high-precision applications requires the differences between these two coordinate frames to be known. Therefore, a lot of effort has been invested into finding a set of transformation parameters to convert coordinates given in PZ-90 to WGS 84 (Misra and Abbot, 1994; Misra et al., 1996; Mitrikas et al., 1998; Rossbach et al., 1996).

The GPS and GLONASS ICDs (GLONASS, 1995; GPS, 1991) give very similar definitions of the WGS 84 and PZ-90 reference frames. Therefore, the differences in orientation between the two frames can be assumed to be small. This enables the application of a seven parameter Helmert transformation to transform coordinates from one frame into another. This seven parameter transformation for a set of coordinates given in a frame *PZ* into a frame *WGS* reads:

$$\begin{matrix} x_{WGS} \\ y_{WGS} \\ z_{WGS} \end{matrix} = \begin{matrix} x_{PZ} \\ y_{PZ} \\ z_{PZ} \end{matrix} + \begin{pmatrix} 1 + \delta s \\ -\delta\omega \\ \delta\psi \end{pmatrix} \begin{matrix} 1 \\ -\delta\omega \\ \delta\psi \end{matrix} \begin{matrix} \delta\omega \\ 1 \\ -\delta\epsilon \end{matrix} \begin{matrix} -\delta\psi \\ \delta\epsilon \\ 1 \end{matrix} \begin{matrix} x_{PZ} \\ y_{PZ} \\ z_{PZ} \end{matrix} \quad (1)$$

with

$\Delta x, \Delta y, \Delta z$ coordinates of the origin of frame *PZ* in frame *WGS*

$\delta\epsilon, \delta\psi, \delta\omega$ differential rotations around the x-, y- and z-axes of the *PZ* frame, respectively, to establish parallelism with the *WGS* frame

δs differential scale change

Neither of the ICDs defines a set of parameters to be used in transforming satellite coordinates. These transformation parameters must be determined separately. This currently is one of the most intensely investigated topics in GPS/GLONASS combination. Different groups of researchers have determined their own sets of parameters that differ from one another like the methods they used to determine these parameters.

Conventional Techniques for the Determination of Transformation Parameters

The attempts to determine the transformation parameters from PZ-90 to WGS 84 used so far (Misra and Abbot, 1994; Misra et al., 1996; Mitrikas et al., 1998; Rossbach et al., 1996) all had one approach in common: They measured or otherwise obtained the coordinates of a given set of points in both coordinate frames, PZ-90 and WGS 84. Afterwards, a set of transformation parameters was calculated that brings the coordinates into coincidence when applied to the coordinates of one of the coordinate frames.

To determine the seven parameters of the coordinate transformation as introduced above, at least seven point coordinates must be known in both frames to obtain seven equations for solving seven unknowns. Since each point in space supplies three coordinates (one each for the x-, y- and z-axes), measuring three points is mathematically sufficient to calculate the desired transformation parameters. However, to have a good quality of the

obtained parameters, it is desired to have coordinates of as many points as possible for reasons of redundancy in the equations. In addition, these points should be globally distributed to extend the validity area of the derived parameters. Otherwise, translational and rotational parameters may not be sufficiently separated from each other. This will result in a set of transformation parameters that is only valid in a specific area of the Earth.

Possible methods of parameter determination can be distinguished by the location of the points whose coordinates are obtained in both systems:

Ground-based techniques: Coordinates of points on the surface of the Earth are made known in both coordinate frames. Usually, either a set of points known in WGS 84 is occupied and measured in PZ-90 or the other way around.

Space-based techniques: Coordinates of satellites at a specified epoch in time are made known in both coordinate frames. Usually, coordinates of GLONASS satellites are obtained from their ephemerides (in PZ-90) and from ground tracking from sites known in WGS 84 .

Each of the ground-based techniques suffers from a disadvantage with respect to the space-based techniques: There are no known points with coordinates known in PZ-90 outside the territory of the former Soviet Union. This makes it nearly impossible to occupy these points with GPS receivers, determine their coordinates in WGS 84 and derive a globally valid set of transformation parameters. On the other hand, there are plenty of points with coordinates known in WGS 84 all around the world. But until recently, there were only a few geodetic quality GLONASS receivers available. These were too few to occupy these points, determine their coordinates in PZ-90 and derive a globally valid set of transformation parameters. Only in 1998, a sufficient number of GPS/GLONASS receivers became available to be used in the IGEX-98 global observation campaign.

Regarding this, the space-based techniques have one major advantage: With only a few GLONASS receivers, broadcast ephemeris data (in the PZ-90 frame) of all GLONASS satellites all around the world can be received, providing global coverage. However, getting GLONASS orbit data in the WGS 84 frame can be expensive. These can be obtained by radar or SLR tracking of the satellites, both of which require a large infrastructure, if global coverage is to be obtained. Therefore, each group of scientists that determined transformation parameters using a space-based technique cooperated closely or was sponsored by an organization that can provide such an infrastructure, e.g. NASA.

A different possibility to determine orbits of GLONASS satellites in the WGS 84 frame is to track the satellites using a network of receivers located at sites surveyed in WGS 84 and then compute the satellite orbits from the range measurements, like IGS does to obtain precise ephemerides of GPS satellites. But again, this requires a sufficient number

of globally distributed GLONASS receivers. A number of IGEX-98 analysis centers are using this technique to obtain precise ephemerides of GLONASS satellites in WGS 84 .

Direct Estimation of Transformation Parameters

As stated above, these different methods of determination of transformation parameters all have in common that coordinates in PZ-90 are calculated for points known in WGS 84 or vice versa. The transformation parameters then are derived from comparing these coordinates in PZ-90 and WGS 84 and trying to bring them into coincidence.

However, given observation sites with WGS 84 coordinates, tracking GLONASS satellites, transformation parameters can also be determined directly from the range measurements themselves, skipping the necessity for determination of the coordinates of the sample point in the PZ-90 frame. This method of parameter determination will be introduced in this paper. This paper furthermore shows the results of this procedure being applied to data of the IGEX-98 measurement campaign.

The principle of direct determination of the transformation parameters is shown for station coordinates given in WGS 84. It can, however, be applied to any other ECEF coordinate frame as well. In the IGEX-98 campaign, coordinates of the observation sites were given in ITRF-96. Thus, the results of this process primarily will be a set of transformation parameters from PZ-90 to ITRF-96. However, ITRF-96 and WGS 84 can be regarded as identical.

The (simplified) pseudorange observation equation from receiver R to satellite S is given by

$$PR_R^S = \rho_R^S + c\delta t_R - c\delta t^S + c T_R^{S,trop} + c T_R^{S,iono} \quad (2)$$

with

- PR_R^S Pseudorange from receiver R to satellite S
- ρ_R^S Geometric distance from R to satellite S
- c Speed of light
- δt_R Receiver clock offset
- δt^S Satellite clock offset
- $T_R^{S,trop}$ Tropospheric path delay between S and R
- $T_R^{S,iono}$ Ionospheric path delay between S and R

The geometric distance is given by

$$\rho_R^S = \sqrt{(x_R - x^S)^2 + (y_R - y^S)^2 + (z_R - z^S)^2} \quad (3)$$

The position vectors of receiver \underline{x}_R and \underline{x}^S in Eq. (3) must be given in the same coordinate frame.

In the given case of IGEX-98 observation sites taking range measurements to GLONASS satellites, the known coordinates of the observation sites are given in WGS 84 , whereas

the coordinates of the GLONASS satellites are determined from ephemeris data and are given in PZ-90. Since both WGS 84 and PZ-90 are Earth-centered Earth-fixed (ECEF) coordinate frames, they rotate along with the Earth. Their orientation therefore is a function of time. More precise, thus, the coordinates of the observation sites are given in WGS 84, as valid at the time of signal reception t_{RX} , and the coordinates of the satellites are given in PZ-90, as valid at the time of signal transmission t_{TX} .

$$\begin{aligned}\underline{x}_R &= \underline{x}_{R,WGS(t_{RX})} \\ \underline{x}^S &= \underline{x}_{PZ(t_{TX})}^S\end{aligned}$$

To obtain the actual geometrical distance from receiver to satellite from Eq. (3), one of these two sets of coordinates must be transformed to the coordinate frame of the other set. Here it is chosen to transform the satellite coordinates to the coordinate frame of the observer. This requires two steps of transformation:

- Transformation from PZ-90 to WGS 84 : $\underline{x}_{PZ(t_{TX})}^S \rightarrow \underline{x}_{WGS(t_{TX})}^S$
- Correction of Earth rotation: $\underline{x}_{WGS(t_{TX})}^S \rightarrow \underline{x}_{WGS(t_{RX})}^S$

Correction of Earth Rotation

While the satellite signal is travelling towards the observer, the Earth - and along with it the Earth-fixed coordinate frame - keeps rotating. During this signal travel time, it rotates by an angle of $\alpha = \rho_R^S \omega_E / c$, where ω_E is Earth's rotation rate. This is a positive rotation around the z-axis. Thus, the satellite coordinates transform by

$$\underline{x}_{WGS(t_{RX})}^S = \begin{bmatrix} 1 & \alpha & 0 \\ -\alpha & 1 & 0 \\ 0 & 0 & 1 \end{bmatrix} \underline{x}_{WGS(t_{TX})}^S \quad (4)$$

for small angles α .

Formulating the geometrical distance between satellite and receiver in the WGS 84 frame at the time of signal reception

$$\rho_R^S = \left[\left(x_{R,WGS(t_{RX})} - x_{WGS(t_{RX})}^S \right)^2 + \left(y_{R,WGS(t_{RX})} - y_{WGS(t_{RX})}^S \right)^2 + \left(z_{R,WGS(t_{RX})} - z_{WGS(t_{RX})}^S \right)^2 \right]^{1/2}$$

and inserting Eq. (4) yields after some modifications

$$\begin{aligned}\rho_R^S &= \frac{\omega_E}{c} \left(x_{R,WGS(t_{RX})} y_{WGS(t_{TX})}^S - y_{R,WGS(t_{RX})} x_{WGS(t_{TX})}^S \right) + \frac{\omega_E^2}{c} \left(x_{R,WGS(t_{RX})} y_{WGS(t_{TX})}^S - y_{R,WGS(t_{RX})} x_{WGS(t_{TX})}^S \right)^2 + \\ &\quad \left(x_{R,WGS(t_{RX})} - x_{WGS(t_{TX})}^S \right)^2 + \left(y_{R,WGS(t_{RX})} - y_{WGS(t_{TX})}^S \right)^2 + \left(z_{R,WGS(t_{RX})} - z_{WGS(t_{TX})}^S \right)^2 \Big]^{1/2} \quad (5)\end{aligned}$$

For deriving Eq. (5), the WGS 84 coordinate frame was used. Of course, Eq. (5) would also be valid in the PZ-90 coordinate frame.

Transformation from PZ-90 to WGS 84

Writing the seven parameter Helmert transformation Eq. (1) in individual coordinates, valid at time t_{TX} , yields:

$$\begin{aligned} x_{WGS(t_{TX})}^S &= x + (1 + \delta s) \left(x_{PZ(t_{TX})}^S + \delta\omega y_{PZ(t_{TX})}^S - \delta\psi z_{PZ(t_{TX})}^S \right) \\ y_{WGS(t_{TX})}^S &= y + (1 + \delta s) \left(-\delta\omega x_{PZ(t_{TX})}^S + y_{PZ(t_{TX})}^S + \delta\epsilon z_{PZ(t_{TX})}^S \right) \\ z_{WGS(t_{TX})}^S &= z + (1 + \delta s) \left(\delta\psi x_{PZ(t_{TX})}^S - \delta\epsilon y_{PZ(t_{TX})}^S + z_{PZ(t_{TX})}^S \right) \end{aligned} \quad (6)$$

Inserting this into Eq. (5) yields the rather lengthy Eq. (7) for the geometric distance between receiver R and satellite S .

$$\begin{aligned} \rho_R^S &= -\frac{\omega_E}{c} \left\{ x_{R,WGS(t_{RX})} \left[y + (1 + \delta s) \left(-\delta\omega x_{PZ(t_{TX})}^S + y_{PZ(t_{TX})}^S + \delta\epsilon z_{PZ(t_{TX})}^S \right) \right] - \right. \\ &\quad \left. y_{R,WGS(t_{RX})} \left[x + (1 + \delta s) \left(x_{PZ(t_{TX})}^S + \delta\omega y_{PZ(t_{TX})}^S - \delta\psi z_{PZ(t_{TX})}^S \right) \right] \right\} + \\ &\quad \frac{\omega_E}{c} \left\{ x_{R,WGS(t_{RX})} \left[y + (1 + \delta s) \left(-\delta\omega x_{PZ(t_{TX})}^S + y_{PZ(t_{TX})}^S + \delta\epsilon z_{PZ(t_{TX})}^S \right) \right] - \right. \\ &\quad \left. y_{R,WGS(t_{RX})} \left[x + (1 + \delta s) \left(x_{PZ(t_{TX})}^S + \delta\omega y_{PZ(t_{TX})}^S - \delta\psi z_{PZ(t_{TX})}^S \right) \right] \right\}^2 + \\ &\quad \left\{ x_{R,WGS(t_{RX})} - \left[x + (1 + \delta s) \left(x_{PZ(t_{TX})}^S + \delta\omega y_{PZ(t_{TX})}^S - \delta\psi z_{PZ(t_{TX})}^S \right) \right] \right\}^2 + \\ &\quad \left\{ y_{R,WGS(t_{RX})} - \left[y + (1 + \delta s) \left(-\delta\omega x_{PZ(t_{TX})}^S + y_{PZ(t_{TX})}^S + \delta\epsilon z_{PZ(t_{TX})}^S \right) \right] \right\}^2 + \\ &\quad \left\{ z_{R,WGS(t_{RX})} - \left[z + (1 + \delta s) \left(\delta\psi x_{PZ(t_{TX})}^S - \delta\epsilon y_{PZ(t_{TX})}^S + z_{PZ(t_{TX})}^S \right) \right] \right\}^2 \quad (7) \end{aligned}$$

Here, the coordinates $x_{R,WGS(t_{RX})}$ are the known station coordinates, given in WGS 84, valid at the time of signal reception. $x_{PZ(t_{TX})}^S$ are the satellite coordinates at the time of signal transmission as obtained from ephemeris data. They are given in the PZ-90 frame, valid at the time of signal transmission. The transformation parameters Δx , Δy , Δz , δs , $\delta\epsilon$, $\delta\psi$, $\delta\omega$ are unknown in this geometrical range in different coordinate frames (Eq. (6)). Inserting this geometrical range into the observation equation Eq. (2), these unknowns can be solved for, provided there is a sufficient number of observations.

However, the receiver clock error δt_R in Eq. (2) is also unknown. The satellite clock error δt^S can be determined from ephemeris data, whereas tropospheric and ionospheric path delays $T_R^{S,trop}$ and $T_R^{S,iono}$ can be modeled. Since GLONASS offers free and unobstructed access to the second frequency, dual-frequency ionospheric corrections can be applied alternatively.

This leaves seven unknown transformation parameters and one unknown receiver clock error to solve for. Thus, with range measurements to eight GLONASS satellites at one observation site, a complete set of transformation parameters could be determined. Besides having eight GLONASS satellites in view is rather unlikely in times of depleted GLONASS constellation, this one observation site will provide a poor geometry to separate origin and orientation parameters. As discussed above, this will lead to a set of

parameters that are only valid at a small area around the observation site. More stations will add more strength to the geometry.

However, each additional observation site does also mean an additional receiver and thus one more receiver clock error as a further unknown. For simultaneous observations at five stations, for example, the total is twelve unknowns. Thus, with two to three observations at each station, it is possible to determine the transformation parameters directly from pseudorange observations.



Figure 1. Distribution of used observation sites.

With seven or more observation sites, only two satellites in view per site are required. This is another bonus of this method for determining the transformation parameters. The conventional method of determining point coordinates in PZ-90 from GLONASS satellite observations, and then comparing these coordinates to known coordinates in WGS 84 , requires at least four satellites visible at a station to calculate station coordinates. This approach of direct estimation of the transformation parameters may work with as little as two observations per site. Depending on the number of stations involved, at some sites only one observation may mathematically be sufficient to get a solution, but this one measurement contributes only to the station clock error.

Equation (7), the geometrical range, and Eq. (2), the observation equation, are non-linear in the unknown transformation parameters. Before trying to solve a system of observation equations, Eq. (7) has to be linearized. Therefore, this equation is expanded into a Taylor series around a set of approximate values $\Delta x_0, \Delta y_0, \Delta z_0, \delta s_0, \delta \varepsilon_0, \delta \psi_0, \delta \omega_0$. This results in a rather lengthy and complicated observation equation. This equation is given in the appendix of this paper.

Given a number of GLONASS satellite observations from a site known in WGS 84, the resulting set of linear observation equations can be solved, using for example, a least-squares adjustment or a Kalman filter.

Observation Data

Measurement data from the IGEX-98 experiment were used to calculate a set of transformation parameters directly from GLONASS range measurements. Sixteen days of observation data from January 1999, taken from 21 globally distributed observation sites, were analyzed. The distribution of observation sites and their coordinates used are given in Figure 1 and Table 1, respectively. Closely spaced observation sites (for example, the wtzg/ntz1 pair) were used alternatively in case there were no observations available for the primary site on a particular day. Thus, not all of the stations were used all the time.

Table 1. ITRF-96 Coordinates of the Observation Sites

Station	Name	x [m]	y [m]	z [m]
3sna	3S Navigation	-2482980.5848	-4696608.3467	3517630.9478
csir	Pretoria	5063683.4628	2723896.1933	-2754444.9755
gatr	Gainesville	738693.0451	-5498293.3041	3136519.5906
godz	Goddard SFC	1130773.8333	-4831253.5816	3994200.4106
herp	Herstmonceux	4033454.7310	23664.4484	4924309.0139
irkz	Irkutsk	-968310.0957	3794414.4427	5018182.1289
khab	Khabarovsk	-2995266.3617	2990444.6917	4755575.9808
lds1	Leeds	3773063.6912	-102444.0029	5124373.4582
mdvz	Mendeleevo	2845461.7803	2160957.5040	5265989.0378
metz	Metsahovi	2892569.9510	1311843.5724	5512634.4596
mtka	Mitaka	-3947762.7194	3364399.8226	3699428.5206
ntz1	Neustrelitz	3718450.4080	863437.7680	5092635.9280
reyz	Reykjavik	2587383.7759	-1043032.7094	5716564.4408
sang	Santiago de Chile	1769719.8283	-5044542.6396	-3468352.4705
sl1x	MIT Lincoln Lab	1513678.5253	-4463031.6196	4283433.5383
str	Stromlo	-4467102.3957	2683039.4598	-3666949.7020
thu2	Thule	538093.6860	-1389088.0068	6180979.1953
tska	Tsukuba	-3957203.2551	3310203.1701	3737704.4658
usnx	US Naval Observatory	1112158.1709	-4842852.8153	3985491.4382
wtzg	Wetzell	4075580.1058	931855.2874	4801568.3246
yarr	Yarragadee	-2389024.5495	5043315.4590	-3078534.1138

Wherever possible, the ionospheric-free linear combination of L1 and L2 measured pseudoranges was used in the estimation of transformation parameters. Where there were not dual-frequency measurements available, the GPS Klobuchar model, adapted to GLONASS frequencies, was used to reduce the ionospheric path delay.

To reduce the influence of measurement noise and multipath, if present, carrier smoothing of the pseudoranges was applied before the linear combination was formed. To compensate for the tropospheric path delay, a simple model was used that is not dependent on actual weather data, but uses empirical weather data, depending on latitude/longitude of the observation site, time of year and time of day. This model is described in (RTCA, 1998).

For each of the sixteen days, daily solutions of the transformation parameters were estimated in a Kalman filter. These daily solutions were averaged to obtain a set of transformation parameters:

	Δx [m]	Δy [m]	Δz [m]	δs [10^{-9}]	$\delta \epsilon$ [10^{-6}]	$\delta \psi$ [10^{-6}]	$\delta \omega$ [10^{-6}]
Average	0.404	0.357	-0.476	-2.614	0.118	-0.058	-1.664
Std. dev.	1.039	1.147	0.456	63.860	0.090	0.112	0.170

These results are consistent with previously released transformation parameters (Misra et al., 1996; Mitrikas et al., 1998; Rossbach et al., 1996) insofar as a rotation around the z-axis on the order of $\delta \omega = -1.6 \cdot 10^{-6} \dots -1.9 \cdot 10^{-6}$ can be regarded as the most significant parameter. Average values of the other parameters are on the order of or even less than the standard deviation of the daily solutions.

To verify these transformation parameters, a selection of the observation data was processed again, this time in positioning mode. The station coordinates in WGS 84 were computed from the GLONASS measurements, where the estimated set of transformation parameters was applied to convert GLONASS satellite positions from PZ-90 to WGS 84 before the computation of station coordinates. Positioning was done in single-point mode, using the ionospheric-free linear combination of carrier-smoothed L1 and L2 pseudoranges, wherever available. Again, daily solutions (for the station coordinates) were computed and averaged.

Daily solutions using the transformation introduced above were close to the solutions using the transformation given in (Rossbach et al., 1996). Distances usually were on the order of 1 m. However, the solutions calculated with the transformation above usually were closer to the known ITRF-96 coordinates of the observation stations. The average deviations from the known position in ITRF-96 using the set of transformation parameters introduced above were smaller than the average deviations resulting from positioning with the set of transformation parameters from (Rossbach et al., 1996). The results showed a slight degradation in the x- and y-coordinates, but also a significant improvement in the z-coordinate. Using the transformation introduced above, the average deviation from the known x- and y-coordinates was slightly larger than with the transformation from (Rossbach et al., 1996). The average deviation in the x-coordinate was 0.327 m with this transformation, compared to 0.229 m using (Rossbach et al.,

1996). In the y-component, the deviations were 0.536 m and 0.225 m, respectively. But for the z-coordinate, the average deviation was significantly smaller (0.836 m compared to 1.397 m with (Rossbach et al.,1996). The overall distance to the known coordinates was reduced from 1.433 m using Rossbach et al. (1996) to 1.046 m.

The slight degradation in the x- and y-coordinates may suggest that there is still room for further improvement, especially in the parameters of origin.

Conclusions

This paper introduced a method of estimating the transformation parameters from PZ-90 to WGS 84 directly from range measurements to GLONASS satellites from observation sites surveyed in WGS 84. Compared to the conventional method of using the GLONASS measurements to compute the station coordinates in PZ-90 and then determine the transformation parameters from the differences in the WGS 84 and PZ-90 coordinates, the method introduced can be performed without the intermediate step. Depending on the number of stations involved, as little as two observations per site are sufficient for the parameter estimation. This is a second advantage over the conventional method, which requires at least four satellites being visible at each site to be able to compute the station coordinates.

Applying this new method to data from the IGEX-98 campaign, a set of transformation parameters was determined to be

$$\begin{array}{rcccl}
 x & 0.404\text{m} & 1 & -1.664 \cdot 10^{-6} & 0.058 \cdot 10^{-6} & x \\
 y & = 0.357\text{m} + (1 - 2.614 \cdot 10^{-9}) & 1.664 \cdot 10^{-6} & 1 & 0.118 \cdot 10^{-6} & y \\
 z_{\text{WGS84}} & -0.476\text{m} & -0.058 \cdot 10^{-6} & -0.118 \cdot 10^{-6} & 1 & z_{\text{PZ-90}}
 \end{array} \quad (8)$$

The estimated set of transformation parameters was compared to previously published estimations and shows a good coincidence with these in the significant parameters.

This set of transformation parameters was applied to observation data from the IGEX-98 campaign to determine WGS 84 coordinates of the observation sites from GLONASS measurements. This yielded an improvement with respect to previously published transformations, especially in the z-coordinate, when comparing the results to the known ITRF-96 station coordinates.

This paper aimed at the introduction of the method of transformation parameter estimation directly from range measurements. The transformation parameters given may be regarded as preliminary values, obtained by means of a rather rough data processing. A more detailed and comprehensive data processing is possible. Still, this method already promises good results.

Acknowledgements

The author wishes to thank all participants in the IGEX-98 campaign, whether as an observation site, data or processing center. Without their effort in collecting and providing GLONASS measurements, this work would not have been possible.

References

- GLONASS (1995). GLONASS Interface Control Document (1995), Coordination Scientific Information Center, Ministry of Defense, Russian Federation.
- GPS (1991). GPS Interface Control Document (ICD-GPS-200), ARINC Research Corporation, July 1991.
- RTCA (1998). Minimum Operational Performance Standards for Global Positioning System/Wide Area Augmentation System Airborne Equipment, Document No. RTCA/DO-229A, June 1998.
- Misra, P.N., R.I. Abbot (1994). SGS-85 - WGS84 Transformation, *manuscripta geodaetica*, Vol. 19, pp. 300–308.
- Misra, P.M., R.I. Abbot, E.M. Gaposchkin (1996). Integrated Use of GPS and GLONASS: PZ-90 – WGS84 Transformation, *Proceedings ION GPS-96*, Kansas City, Sept. 17-20, 1996, pp.307-314, Inst. of Navigation.
- Mitrikas, V. V., S. G. Revnivykh, E. V. Bykhanov (1998). WGS84/PZ-90 Transformation Parameters Determination Based on Laser and Ephemeris Long-Term GLONASS Orbital Data Processing, *Proceedings ION GPS-98*, Nashville, Sept. 15-18, 1998 pp. 1625-1635, Inst. of Navigation.
- Rossbach, U., H. Habrich, N. Zarraoa (1996). Transformation Parameters Between PZ-90 and WGS84, *Proceedings ION GPS-96*, Kansas City, Sept. 17-20, 1996, pp. 279-285.

Appendix

The linearized observation equation for the direct determination of PZ-90 / WGS 84 transformation parameters from GLONASS observations reads:

$$\begin{aligned}
PR_R^S - \rho_{R,0}^S + c\delta t^S - c T_R^{S,trop} - c T_R^{S,iono} = \\
\left. \frac{\rho_R^S}{x_0} \right| (x - x_0) + \left. \frac{\rho_R^S}{y_0} \right| (y - y_0) + \left. \frac{\rho_R^S}{z_0} \right| (z - z_0) + \left. \frac{\rho_R^S}{\delta s_0} \right| (\delta s - \delta s_0) + \\
\left. \frac{\rho_R^S}{\delta \varepsilon_0} \right| (\delta \varepsilon - \delta \varepsilon_0) + \left. \frac{\rho_R^S}{\delta \psi_0} \right| (\delta \psi - \delta \psi_0) + \left. \frac{\rho_R^S}{\delta \omega_0} \right| (\delta \omega - \delta \omega_0) + c\delta t_R \\
\left. \frac{\rho_R^S}{x_0} \right| = \frac{\omega_E}{c} y_{R,WGS(t_{RX})} - \frac{1}{S_0} \frac{\omega_E^2}{c} s_0 y_{R,WGS(t_{RX})} + \xi_0 \\
\left. \frac{\rho_R^S}{y_0} \right| = -\frac{\omega_E}{c} x_{R,WGS(t_{RX})} + \frac{1}{S_0} \frac{\omega_E^2}{c} s_0 x_{R,WGS(t_{RX})} + \nu_0 \\
\left. \frac{\rho_R^S}{z_0} \right| = -\frac{1}{S_0} \zeta_0 \\
\left. \frac{\rho_R^S}{\delta s_0} \right| = -\frac{\omega_E}{c} \left[x_{R,WGS(t_{RX})} \left(-\delta \omega_0 x_{PZ(t_{TX})}^S + y_{PZ(t_{TX})}^S + \delta \varepsilon_0 z_{PZ(t_{TX})}^S \right) - \right. \\
\left. y_{R,WGS(t_{RX})} \left(x_{PZ(t_{TX})}^S + \delta \omega_0 y_{PZ(t_{TX})}^S - \delta \psi_0 z_{PZ(t_{TX})}^S \right) \right] + \\
\frac{1}{S_0} \frac{\omega_E^2}{c} s_0 \left[x_{R,WGS(t_{RX})} \left(-\delta \omega_0 x_{PZ(t_{TX})}^S + y_{PZ(t_{TX})}^S + \delta \varepsilon_0 z_{PZ(t_{TX})}^S \right) - \right. \\
\left. y_{R,WGS(t_{RX})} \left(x_{PZ(t_{TX})}^S + \delta \omega_0 y_{PZ(t_{TX})}^S - \delta \psi_0 z_{PZ(t_{TX})}^S \right) \right] - \\
\xi_0 \left(x_{PZ(t_{TX})}^S + \delta \omega_0 y_{PZ(t_{TX})}^S - \delta \psi_0 z_{PZ(t_{TX})}^S \right) - \nu_0 \left(-\delta \omega_0 x_{PZ(t_{TX})}^S + y_{PZ(t_{TX})}^S + \delta \varepsilon_0 z_{PZ(t_{TX})}^S \right) - \\
\zeta_0 \left(\delta \psi_0 x_{PZ(t_{TX})}^S - \delta \varepsilon_0 y_{PZ(t_{TX})}^S + z_{PZ(t_{TX})}^S \right) \left. \right\} \\
\left. \frac{\rho_R^S}{\delta \varepsilon_0} \right| = (1 + \delta s_0) \left[-\frac{\omega_E}{c} x_{R,WGS(t_{RX})} z_{PZ(t_{TX})}^S + \frac{1}{S_0} \frac{\omega_E^2}{c} s_0 x_{R,WGS(t_{RX})} z_{PZ(t_{TX})}^S - \nu_0 z_{PZ(t_{TX})}^S + \xi_0 y_{PZ(t_{TX})}^S \right] \\
\left. \frac{\rho_R^S}{\delta \psi} \right| = (1 + \delta s_0) \left[-\frac{\omega_E}{c} y_{R,WGS(t_{RX})} z_{PZ(t_{TX})}^S + \frac{1}{S_0} \frac{\omega_E^2}{c} s_0 y_{R,WGS(t_{RX})} z_{PZ(t_{TX})}^S + \xi_0 z_{PZ(t_{TX})}^S - \zeta_0 x_{PZ(t_{TX})}^S \right] \\
\left. \frac{\rho_R^S}{\delta \omega_0} \right| = (1 + \delta s_0) \frac{\omega_E}{c} \left(x_{R,WGS(t_{RX})} x_{PZ(t_{TX})}^S + y_{R,WGS(t_{RX})} y_{PZ(t_{TX})}^S \right) - \\
\frac{1}{S_0} \frac{\omega_E^2}{c} s_0 \left(x_{R,WGS(t_{RX})} x_{PZ(t_{TX})}^S + y_{R,WGS(t_{RX})} y_{PZ(t_{TX})}^S \right) + \xi_0 y_{PZ(t_{TX})}^S + \nu_0 x_{PZ(t_{TX})}^S
\end{aligned}$$

with

$$\begin{aligned}
S_0 &= \sqrt{\frac{\omega_E}{c}^2 s_0^2 + \xi_0^2 + \mathbf{u}_0^2 + \zeta_0^2} \\
s_0 &= x_{R,WGS(t_{RX})} \left[y_0 + (1 + \delta s_0) \left(-\delta\omega_0 x_{PZ(t_{TX})}^S + y_{PZ(t_{TX})}^S + \delta\psi_0 z_{PZ(t_{TX})}^S \right) \right] - \\
&\quad y_{R,WGS(t_{RX})} \left[x_0 + (1 + \delta s_0) \left(x_{PZ(t_{TX})}^S + \delta\omega_0 y_{PZ(t_{TX})}^S - \delta\epsilon_0 z_{PZ(t_{TX})}^S \right) \right] \\
\xi_0 &= x_{R,WGS(t_{RX})} - x_0 - (1 + \delta s_0) \left(x_{PZ(t_{TX})}^S + \delta\omega_0 y_{PZ(t_{TX})}^S - \delta\epsilon_0 z_{PZ(t_{TX})}^S \right) \\
\mathbf{u}_0 &= y_{R,WGS(t_{RX})} - y_0 - (1 + \delta s_0) \left(-\delta\omega_0 x_{PZ(t_{TX})}^S + y_{PZ(t_{TX})}^S + \delta\psi_0 z_{PZ(t_{TX})}^S \right) \\
\zeta_0 &= z_{R,WGS(t_{RX})} - z_0 - (1 + \delta s_0) \left(\delta\epsilon_0 x_{PZ(t_{TX})}^S - \delta\psi_0 y_{PZ(t_{TX})}^S + z_{PZ(t_{TX})}^S \right)
\end{aligned}$$

Analytical SRP Model for GLONASS: Initial Results

Marek Ziebart

Applied Geodesy Research Unit, School of Surveying, University of East London,
Longbridge Road, Dagenham, Essex, RM8 2AS, UK

Abstract

Solar radiation pressure (SRP) is a significant perturbing acceleration on the GLONASS orbit. Although the effects of SRP on an orbit can be estimated empirically with great precision for highly redundant solutions, analytical models are useful for reducing the number of parameters in a solution, and for data processing where fewer observations are available. However, accurate analytical models can be difficult to compute for spacecraft of complex shape, such as the GLONASS IIV satellite. This is principally due to the effects of spacecraft components shadowing each other, and because of secular and other periodic variations, possibly due to attitude control limitations and weathering of the spacecraft materials. This paper discusses a new approach to computing analytical SRP models. The photon flux is simulated using a pixel array. The illumination of the spacecraft and subsequent reflection of the light is calculated using ray tracing algorithms. The summed accelerations are decomposed along the spacecraft X and Z axes for each Earth-probe-Sun angle, and a Fourier series is fitted to the data points to form the model, in a similar fashion to the GPS ROCK models. The resulting model is tested by numerical integration of the spacecraft dynamic model, using a truncated Earth gravity field, as well as solar and lunar gravity. IGEX-98 precise orbit data are used for initial conditions and for analysis of residuals. The software allows the spacecraft to be perturbed from its nominal attitude to simulate Y-bias and the magnitude of scaling factors for the modeled acceleration along the X and Z axes. The initial results for models and testing are presented.

Introduction

The surface area of the GLONASS IIV solar panels (23.616m^2 , cp. GPS block II panels: 10.866m^2) (Fliegel et al, 1992; GEOZUP, 1998) makes it intuitively obvious that solar radiation pressure (SRP) is a significant perturbing acceleration on the GLONASS orbit. Although the effects of SRP on an orbit can be estimated empirically with great precision for highly redundant solutions (Beutler et al., 1994), analytical models are useful for reducing the number of parameters in a solution, for data processing where fewer observations are available and for interpolating to intermediate epochs when using precise orbits. Furthermore, analytical models enable greater insight into the physical processes. However, accurate analytical models can be difficult to compute for spacecraft of complex shape, such as the GLONASS IIV satellite (see Figure 1). This is principally due to the effects of spacecraft components shadowing each other, and because of secular and other periodic variations, possibly due to attitude control limitations (Kuang et al., 1996) and weathering of the spacecraft materials. Furthermore, accurate data for the spacecraft materials and dimensions are not always available.

The objective for this study was to develop a method for computing analytical SRP models for spacecraft of complex shape. Thereafter, apply the algorithm to the GLONASS IIV satellite and test the model.

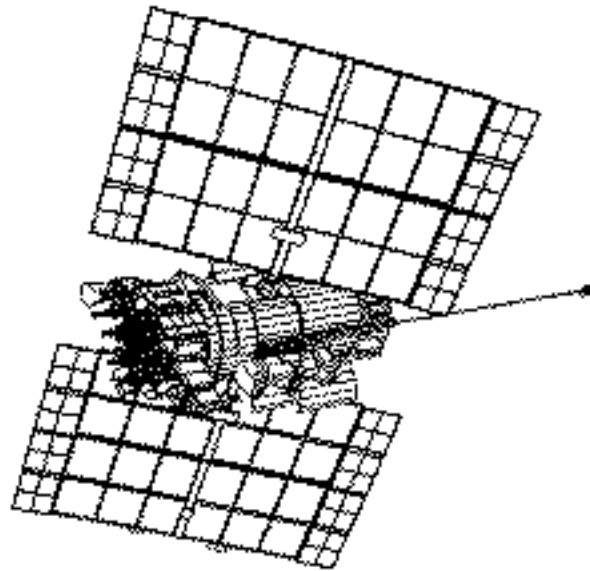


Figure 1. GLONASS IIV spacecraft.

Method

Algorithm for Computing the SRP Model

The spacecraft structure is broken down into a composite of regular and irregular polygons bound within planar surfaces. The software reads a user defined file of component vertices, in a body-fixed coordinate system, and computes the equation of the plane of, and the normal to, each component. Cylindrical components are tessellated by the software into thin, planar strips. The file also includes the specular and reflectivity coefficients for the surface materials.

The photon flux is simulated with a pixel array. This is a grid of small rectangles in a plane orthogonal to the Sun-spacecraft vector. The user specifies the resolution of the array. See Figure 2. Each pixel is converted to a ray by adding the normalised Sun-spacecraft vector to the pixel coordinates. This ray is then projected towards the spacecraft and tested for intersection with the spacecraft components.

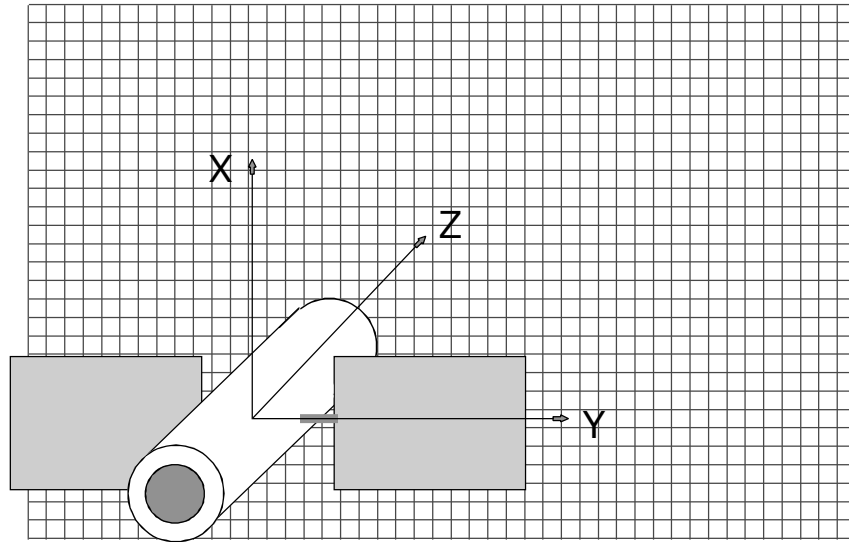


Figure 2. Body-fixed coordinate system and pixel array.

The intersection test works as follows. For each spacecraft component the equation of the plane is calculated. If the ray is not parallel to the plane the intersection point of the plane and the ray is found. A point-in-polygon test determines whether the intersection point is within the limits of the spacecraft component. See Figure 3. If the spacecraft component can be intersected by the ray, the length of the vector from the centre of the pixel to the intersection point is calculated. This is carried out for all spacecraft components which the ray intersects. The intersected component with the shortest associated ray is the surface struck by the light represented by the pixel.

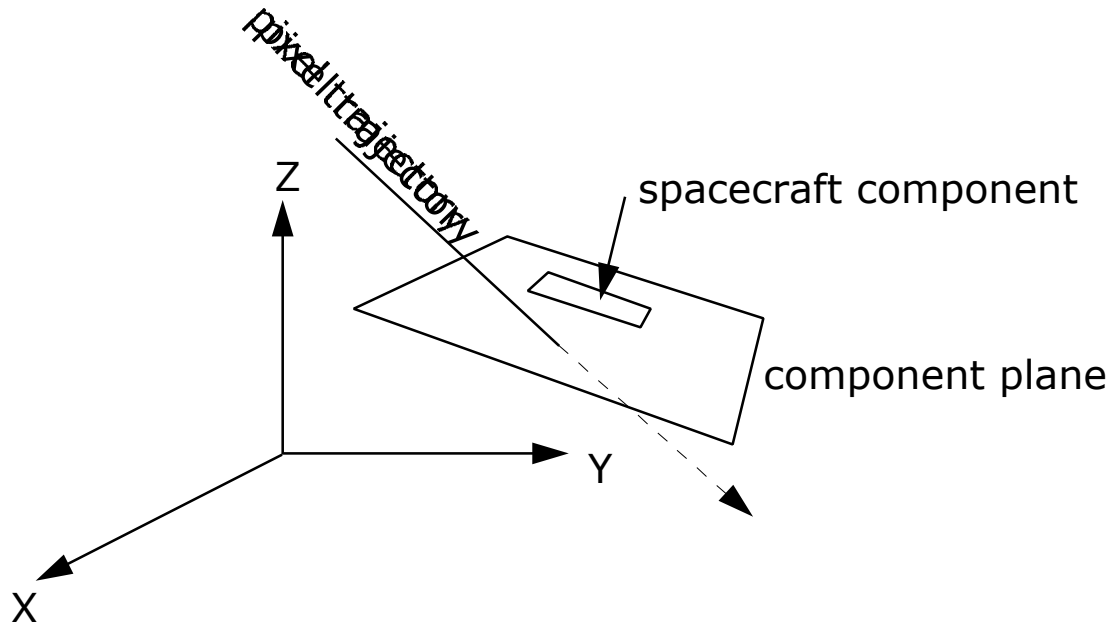


Figure 3. Pixel trajectory intersects component plane.

The reflectivity and specularity coefficients of the struck component, and the angle between the normal to the surface and the ray, are used to calculate the force due to the light both normal and tangential to the surface. Hence, these forces are resolved into body-fixed axis components.

This process is carried out for all the pixels in the array, and the accelerations are added together. This computes the SRP acceleration on the spacecraft for one Sun-spacecraft vector. The user specifies a rotation angle, and this is used to rotate the pixel array about the spacecraft Y-axis, simulating a new Sun-spacecraft vector. Any spacecraft component that changes in orientation with respect to the body-fixed axes as the Sun-spacecraft vector changes is adjusted accordingly. The integration over the pixel array is carried out again. The pixel array is rotated in steps of the rotation angle until 360° has been swept out. This produces a set of data points corresponding to the SRP acceleration on the spacecraft at a set of unique angles of incidence.

A Fourier series is fitted to the data for the spacecraft X- and Z-axes, using the so-called EPS (Earth-probe-Sun) angle as the independent variable (conventional models assume that the spacecraft Y-axis is parallel to the solar panels and hence normal to the photon flux direction, therefore, in theory, there will be no Y-component due to SRP) (Beutler, 1996). Hence, knowing the positions of the spacecraft and the Sun at a particular epoch, the series can be used to calculate the acceleration of the spacecraft due to SRP.

Orbit Integration

The model is tested by calculating the spacecraft trajectory using a dynamic model alone (that is, the trajectory is not constrained by range measurements from reference station receivers or SLR). The initial conditions are taken from the IGEX-98 precise orbits, and the resulting trajectory is compared to the statistically determined trajectory at 15 minute intervals.

In order to incorporate the developed SRP models the integrator was written by the author. At this stage the dynamic model consists of:

- 1) spherical harmonic coefficient model of Earth gravity to degree and order 4 (EGM96)
- 2) solar gravity
- 3) lunar gravity
- 4) custom SRP model

Because of the limited gravity field expansion the results for this study are given over three hour integration periods, that is, arc lengths of approximately 35,000km.

The integrator uses a Runge-Kutta four-step procedure and Cowell's method. Given the low eccentricity of the GLONASS orbit and the slow variation of the dynamic parameters this should give adequate results.

Results

The results are calculated by differencing the integrated trajectory (using various force models) with the CODE precise trajectory.

The results presented are for GLONASS PR4, over a three hour trajectory starting from 1998 10 26 0h 0m 0s UTC. These results are typical for the arcs integrated so far in the study, which are all from the same day. The model assumes that the spacecraft thermofolds are in the closed position.

The first set, Figures 4-6, contrasts the integrated trajectory derived from the available gravitational force models alone (Earth degree and order 4, solar and lunar point mass gravity) with the dynamic model using the gravitational forces and the analytical SRP model. The residuals are in the ECEF coordinate system.

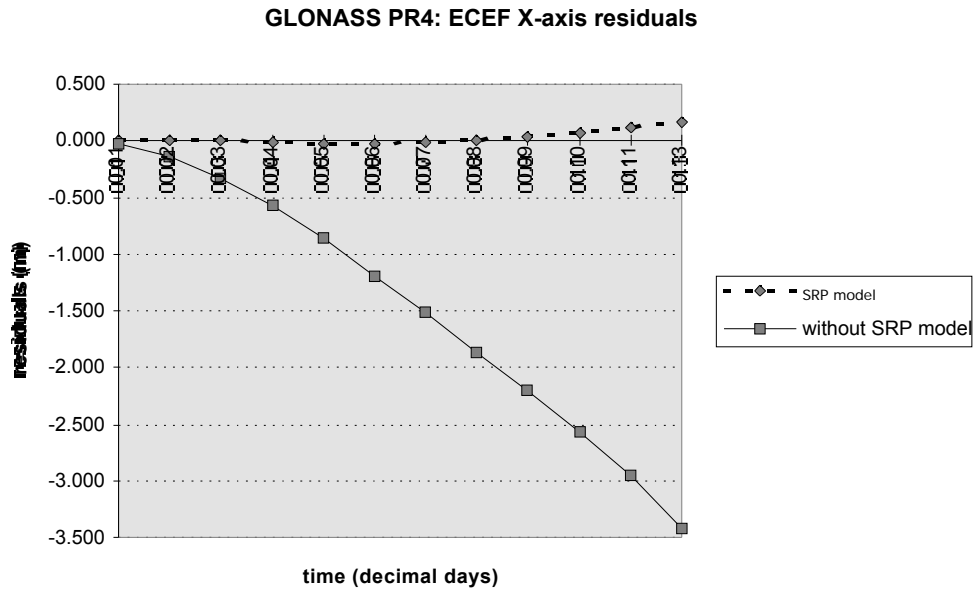


Figure 4. X-axis residuals.

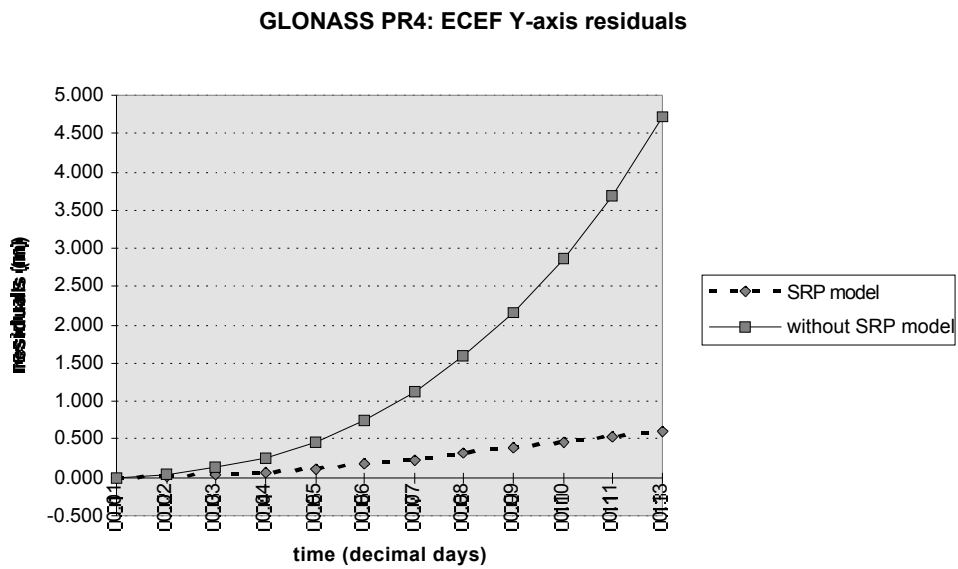


Figure 5. Y-axis residuals.

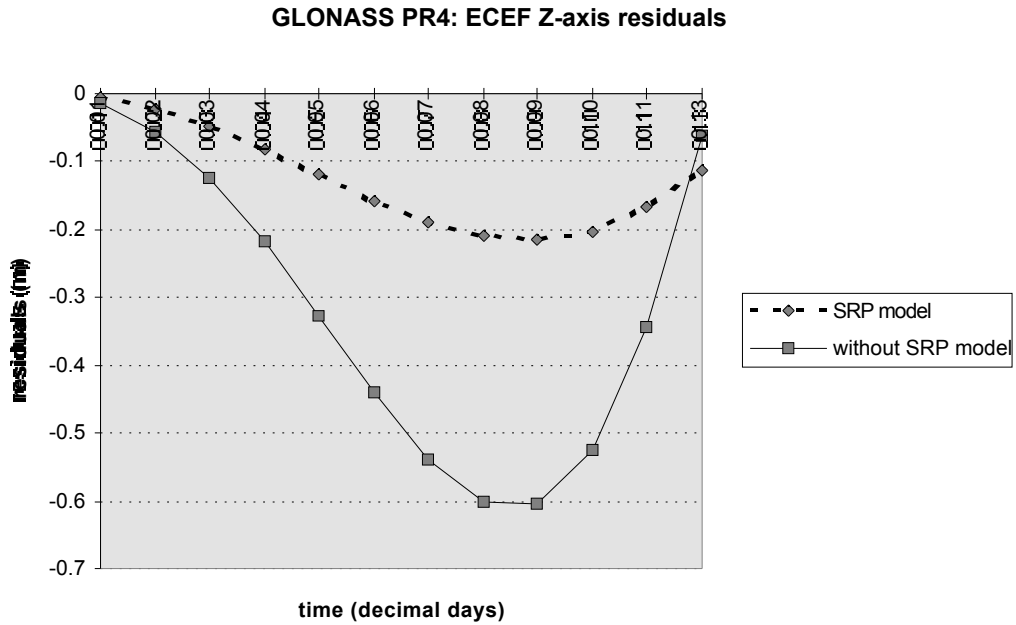


Figure 6. Z-axis residuals.

Figure 7 compares the residuals for the SRP model trajectory in the ECEF X, Y and Z axes.

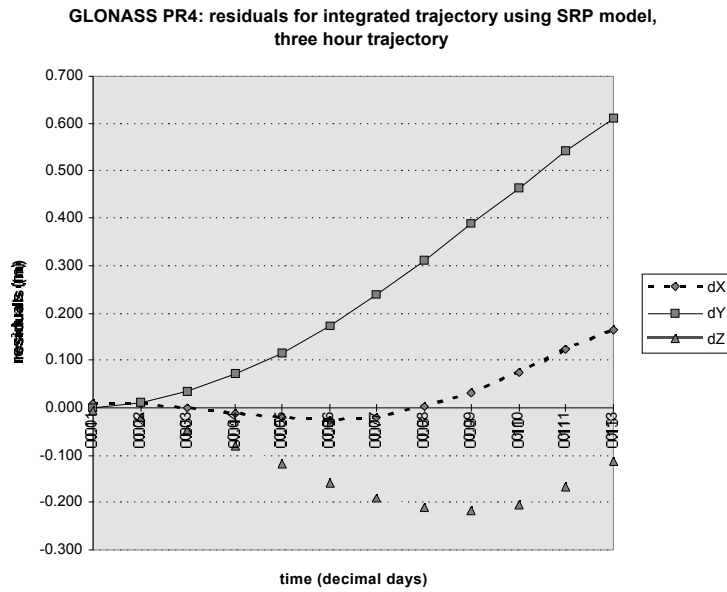


Figure 7. Residuals for integrated trajectory using SRP model, 3-hour trajectory

Discussion

To accurately assess the analytical SRP model by means of orbit integration would require complete modelling of all other non-negligible forces acting on the spacecraft, as well as a known reference trajectory with no errors. As the GLONASS constellation is in a lower orbit compared to GPS it is more sensitive to higher order gravity terms in the Earth gravity field spherical harmonic expansion, although the ground track repeat pattern for GPS can cause resonance effects which would be much smaller for GLONASS (the GPS ground track repeats daily, to a first approximation, whereas GLONASS repeats every eight days). The author intends to extend the gravity field modelling for the orbit integration to degree and order 10, and to include contributions due to the gravity of Jupiter, Saturn, Mars and Venus, as well as tidally induced variations to the potential. Whilst this is readily achievable there are more problematic areas:

- 1) due to the size of the solar panels, and the average altitude of the orbit, albedo and atmospheric drag may be non-negligible. Both of these are difficult to model accurately due to the chaotic nature of the environment variables.
- 2) thermal re-radiation
- 3) the position of the spacecraft thermofolds as a function of time or temperature
- 4) assumptions about the surface material properties (this model has assumed weathered aluminium for most of the bus components, and solar panel materials identical to GPS counterparts)
- 5) the precise attitude of the spacecraft (noon-day turns, accuracy of the boresight pointing and sensing of the Sun's position)
- 6) lastly, unpredictable yawing of the spacecraft during eclipse periods

Having outlined all these problem areas it is clear from the results that the initial SRP model developed for this study is a significant improvement to the dynamic model for the spacecraft. The modelling algorithm successfully copes with the complexity of the spacecraft form and allows the investigator to vary the modelling parameters to assess improvements in accuracy. These might include varying the resolution of the pixel array, increasing the number of points at which the acceleration on the spacecraft is computed (the model used in the study used a pixel resolution of 10mm and calculated the acceleration at intervals of 36° in the EPS angle), and setting higher precision for the Fourier coefficients as well as increasing the number of terms in the series. For precise orbit applications the estimation of empirical scaling factors would compensate for most of problems 1-5. Problem 6 can be avoided by simply screening for periods of eclipse. The analytical model itself can be improved by the following:

- adapt the SRP modelling algorithm to take into account the light reflected from one spacecraft component onto another (work in progress)
- if the thermofold position is related to the central bus temperature some attempt at modelling may be feasible

- assess secular and periodic variations in the solar irradiance value by using the empirical SRP scaling factor data provided by IGS global network analysis of GPS.

Conclusions

A new algorithm for computing analytical solar radiation pressure models has been developed. The principal advantage of this pixel array algorithm is that it handles complex shapes in an efficient and accurate manner, particularly with respect to accounting for the shadowing of components. The algorithm has been successfully applied to the GLONASS IIv spacecraft. Integration of the spacecraft second order differential equation of motion, incorporating the developed SRP model, over a three hour trajectory, results in residuals of the order of 0.5m when compared to the precise orbit produced by CODE. Further developments have been outlined to improve and test this model over longer arcs.

References

- Beutler, G., E. Brockmann, W. Gurtner, U. Hugentobler, L. Mervart, M. Rothacher, A. Verdun (1994). Extended Orbit Modeling Techniques at the CODE Processing Centre of the International GPS Service for Geodynamics (IGS): Theory and Initial Results, *manuscripta geodaetica*, Vol. 19, pp. 367-386.
- Beutler, G. (1996). GPS Satellite Orbits, in *GPS for Geodesy*, A. K. Kleusberg and P.J.G. Teunissen, (Eds.), pp. 37-101, Springer-Verlag.
- Bock, Y. (1996). Reference Systems, in *GPS for Geodesy*, A. K. Kleusberg and P.J.G. Teunissen, (Eds.), pp. 4-35, Springer-Verlag.
- Fliegel, H.F., T.E.Gallini, E.R.Swift (1992). Global Positioning System Radiation Force Model for Geodetic Applications, *Journal of Geophysical Research*, Vol. 97, No. B1, pp. 559-568.
- Fliegel, H. F., T.E. Gallini (1996). Solar Force Modeling of Block IIR Global Positioning System Satellites, *Journal of Spacecraft and Rockets*, Vol. 33, No. 6, pp. 863-866.
- GEOZUP (1998). GLONASS spacecraft description, <http://www.mcc.rsa.ru/IACKVO/igex98.htm>.
- Habrich, H. (1998). Experiences of the BKG in Processing GLONASS and Combined GLONASS/GPS Observations. http://www.ifag.de/kartographie/GF/glo_proc/glo_proc.html, Federal Agency for Cartography and Geodesy: 11.
- Kuang, D., H.J.Rim, B.E.Schutz, P.A.M.Abusali (1996). Modeling GPS Satellite Attitude Variation for Precise Orbit Determination, *Journal of Geodesy*, Vol. 70, pp. 572-580.

- Taylor, G. (1994). Point in Polygon Test, *Survey Review*, Vol. 32, Oct. 1994, pp. 479-484.
- Vigue, Y., S.M. Lichten, R.J. Muellerschoen, G. Blewitt, M.B. Heflin (1994). Improved GPS Solar Radiation Pressure Modeling for Precise Orbit Determination, *Journal of Spacecraft and Rockets*, Vol. 31, No. 5, pp. 830-833.
- Vigue, Y., B.E. Schutz, P.A.M. Abusali (1994). Thermal Force Modeling for Global Positioning System Satellites Using the Finite Element Method. *Journal of Spacecraft and Rockets*, Vol. 31, No. 5, pp. 855-859.